Universidade de Aveiro Departamento de Química
2013

Ana Rita Parente Figueiredo

Novos nanocompósitos de celulose bacteriana preparados por polimerização *in situ*

Universidade de Aveiro Departamento de Química
2013

Ana Rita Parente Figueiredo

Novos nanocompósitos de celulose bacteriana preparados por polimerização *in situ*

Novel bacterial cellulose nanocomposites prepared through *in situ* polymerization

Dissertação apresentada à Universidade de Aveiro para cumprimento dos requisitos necessários à obtenção do grau de Mestre em Biotecnologia Molecular, realizada sob a orientação científica do Doutor Armando Jorge Domingues Silvestre, Professor Associado do Departamento de Química da Universidade de Aveiro, e da Doutora Carmen Sofia da Rocha Freire Barros, Investigadora Auxiliar do Centro de Investigação em Materiais Cerâmicos e Compósitos (CICECO), Universidade de Aveiro.

o júri

Presidente

Prof. Doutor José António Teixeira Lopes da Silva
Professor auxiliar do Departamento de Química da Universidade de Aveiro

Prof. Doutor Jorge Fernando Jordão Coelho
Professor auxiliar da Faculdade de Ciências e Tecnologia da Universidade de Coimbra

Prof. Doutor Armando Jorge Domingues Silvestre
Professor associado com agregação do Departamento de Química da Universidade de Aveiro

Prof. Doutora Carmen Sofia da Rocha Freire Barros
Investigadora auxiliar do Centro de Investigação em Materiais Cerâmicos e Compósitos (CICECO), da Universidade de Aveiro

Agradecimentos

Aproveito esta oportunidade para demonstrar o meu reconhecimento a todos aqueles que tornaram possível a realização deste trabalho:

Aos meus orientadores Professor Doutor Armando Silvestre e à Doutora Carmen Freire, pela ajuda e constante disponibilidade ao longo deste trabalho.

À Andrea Figueiredo pelo seu rigor científico, disponibilidade e ajuda na realização deste trabalho.

Ao Nuno Silva pela disponibilidade e ajuda na realização dos ensaios mecânicos.

À Professora Doutora Adelaide Almeida pela disponibilidade para a realização dos ensaios de atividade antimicrobiana dos materiais no departamento de biologia e pelo apoio prestado.

À Professora Doutora Virgília Silva, do Departamento de Biologia, pela cedência do luminómetro.

Aos colegas do grupo de Materiais Macromoleculares e Lenhocelulósicos pelo bom ambiente e apoio que tornaram a realização deste trabalho mais fácil.

À minha família pelo carinho e motivação, sem os quais a realização deste trabalho não teria sido possível.

Palavras-chave Celulose bacteriana, nanocompósitos, poly(metacrilato de 2-aminoetilo) (PAEM), polimerização *in situ*, atividade antibacteriana, *Escherichia coli* bioluminescente

Resumo

A celulose é o polissacarídeo mais abundante na Natureza, sendo o principal componente estrutural das plantas, e com uma importância industrial elevada principalmente na indústria papeleira e têxtil. Para além das plantas, a celulose é também produzida por algumas bactérias sendo designada de celulose bacteriana (BC). A BC apresenta propriedades únicas, como a elevada retenção de água, resistência mecânica, biodegradabilidade e biocompatibilidade, que tem atraído enorme atenção em diversas áreas. Uma das principais aplicações da BC é o desenvolvimento de nanocompósitos, com aplicações desde a área biomédica, como moldes para engenharia de tecidos, até áreas mais técnicas, como materiais de embalagem.

Assim, este trabalho descreve a preparação de nanocompósitos de celulose bacteriana e poli(metacrilato de 2-aminoetilo) (PAEM) por polimerização radicalar *in situ*, com quantidades variáveis de *N,N*-metilenobis(acrilamida) (MBA) como reticulande. Deste processo resultaram filmes nanocompósitos mais transparentes que a BC com propriedades mecânicas melhoradas assim como maior estabilidade térmica, em relação aos polímeros puros. Para além disso, os nanocompósitos apresentam elevada capacidade de reabsorção de água após secos e cristalinidade reduzida, relativamente à BC pura, devido à incorporação do polímero amorfo.

A atividade antibacteriana nos nanocompósitos foi também avaliada utilizando *E. coli* bioluminescente, tendo-se verificado que apenas o nanocompósito não reticulado (BC/PAEM) apresenta actividade antibacteriana.

Keywords Bacterial cellulose, nanocomposites, poly(2-aminoethyl methacrylate) (PAEM), *in situ* polymerization, antibacterial activity, bioluminescent *Escherichia coli*

Abstract

Cellulose is the most abundant polysaccharide in Nature being the main structural component in plants, and having a high economic importance, namely in paper and textile industries. Besides plants, cellulose is also produced by some bacteria, the so called bacterial cellulose (BC). BC has unique properties such as high water holding ability, mechanical strength, biodegradability and biocompatibility; that attracted its attention towards several fields. One of the BC applications is the development of nanocomposite materials, with applications ranging from biomedical field, as tissue scaffolds, to more technical fields such as packaging materials.

So, the aim of this work was to prepare bacterial cellulose-poly(2-aminoethyl methacrylate) (PAEM) nanocomposites by *in situ* radical polymerization, using variable amounts of *N*,*N*-methylenebis(acrylamide) (MBA) as crosslinker agent. Several nanocomposite films were prepared, showing to be significantly more transparent than BC, with improved mechanical properties and thermal stability, in comparison with the pristine polymers. Furthermore, the nanocomposite materials show high swelling ability in water after drying as well as decreased crystallinity, in comparison with pure BC, as a result of the incorporation of amorphous polymer.

The antibacterial activity of the nanocomposites prepared was also assessed towards bioluminescent E. coli from which only the non-crosslinked nanocomposite (BC/PAEM) showed to have antibacterial activity.

Index

List of figures

List of tables

List of abbreviations

AA	Acrylic acid
AEM	2-Aminoethyl methacrylate
BA	*n*-Butyl acrylate
BC	Bacterial cellulose
CFU	Colony-forming units
DP	Degree of polymerization
EDEMA	2-Ethoxyethyl methacrylate
EHA	2-Ethylhexyl methacrylate
FESEM	Field Emission Scanning Electron Microscopy
FTIR	Fourier Transform Infrared Spectroscopy
GMMA	Glyceryl methacrylate
HEMA	2-Hydroxyethyl methacrylate
MBA	*N,N*-methylenebis(acrylamide)
MMA	Methyl methacrylate
NFC	Nanofibrillated cellulose
NMR	Nuclear Magnetic Resonance
NVP	N-vinyl pyrrolidone
PAEM	Poly(2-aminoethyl methacrylate)
PBA	Poly(butyl acrylate)
PBS	Phosphate Buffer Saline
PEG	Poly(ethylene glycol)
PEGDA	Polyethylene glycol diacrylate
PHB	Poly(3-hydroxybutyrate)
PHEMA	Poly(2-Hydroxyethyl methacrylate)
PLA	Poly(lactic acid)
PMMA	Poly(methyl methacrylate)
RLU	Relative light units
SEM	Scanning Electron Microscopy
TEM	Transmission Electron Microscopy
TGA	Thermogravimetric analysis
TPS	Thermoplastic starch
TSB	Tryptic Soy Broth
XRD	X-ray diffraction

1. Introduction

1.1. The context

Renewable resources have been explored by humankind long before the discovery of its fossil counterparts. However, the boom of petroleum-based materials caused the decline of the use of chemicals, materials and fuels based on renewable resources [1,2]. Nevertheless, the limited supply and increasing cost of fossil resources, along with the growing environmental awareness, once again drew attention into the production of a wide range of chemicals, fuels and materials from renewable origin [1–3].

In the last decades, tremendous efforts have been devoted to the production of novel, environmentally friendly and sustainable materials based on renewable resources. Among the renewable feedstock's that can be used to produce such materials, plants derived biomass is by far the most important source; and, among the plant components, polysaccharides are considered as the most interesting fraction because of their abundance, chemical versatility and (for materials applications) physical properties [2,4].

Cellulose, the most abundant polysaccharide in nature, with about $1{,}5 \times 10^{12}$ tons produced each year, has a high economic importance, namely in the textile and paper industries [2,5]; and is one of the most extensively investigated polysaccharides for composite materials preparation.

The discovery of nanocellulose forms, namely nanofibrillated cellulose (NFC) and bacterial cellulose (BC), opened new perspectives for the development of sustainable nanocomposite materials due to the improved and innovative properties that these cellulose forms can impart to the materials, namely improved mechanical properties and transparency [6].

Bacterial cellulose nanocomposites can be prepared by different approaches, namely: (1) introduction of polymers or other components during BC biosynthesis, (2) blending with other polymeric materials (with or without previous chemical modification of BC), and (3) *in situ* polymerization of different monomers within the BC network.

In this context, the aim of the present work is to prepare and characterize novel nanocomposite materials based on bacterial cellulose and acrylic polymers, specifically poly(2-aminoethyl methacrylate) (PAEM), prepared by the conventional *in situ* radical polymerization of 2-aminoethyl methacrylate (AEM) inside the BC network. The

obtained nanocomposites were characterized in terms of its structure, morphology, thermal stability, mechanical properties and antibacterial activity.

1.2. Plant cellulose

Plants are the dominant source of cellulose, in which this biopolymer is the principal structural element of primary cell walls (Figure 1) [7–11].

Cotton and wood are the most economically important cellulose sources, being these raw materials used for textile and paper industries, respectively [12].

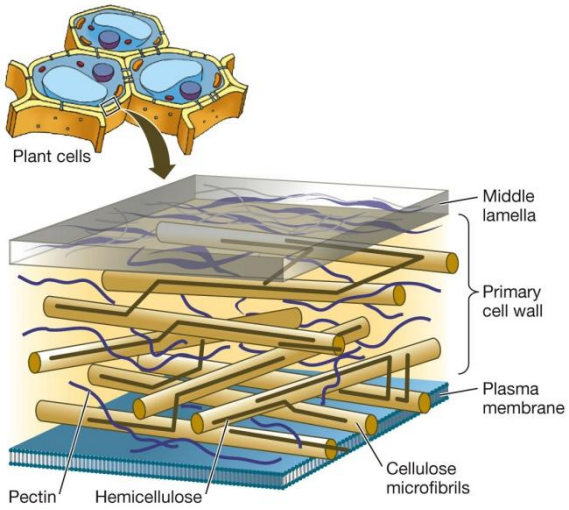

Figure 1 – Schematic representation of plant cell wall and its components (reproduced from [13]).

Cotton seed hairs contain cellulose in an almost pure form [12]. In wood, on the other hand, cellulose is associated with other polymers such as lignin, hemicelluloses and pectins [7,10], creating a natural composite material [12]. Lignin is bound to cellulose fibers, promoting their cohesion, as well as to hemicelluloses contributing to the stem mechanical resistance against gravity forces and wind and also keeping water in the fibers [7]. Pectins also promote strength and support to the plants and influence various cell wall properties such as porosity, surface charge, pH, and ion balance [14].

As mentioned before, cellulose may be obtained in an almost pure form from cotton, however its isolation from wood involves a series of chemical and physical purification processes, such as for example those used in the pulp and paper industry [15].

1.2.1. Molecular and supramolecular structure of cellulose

Cellulose is a white fiber-like and odorless material consisting of a linear homopolymer of β-D-glucopyranose units linked by β-(1→4) glycosidic linkages (Figure 2) [5,7,16–18]. In order to provide acetal bridges with its preferred bond angles, every second ring is rotated 180º. This way, two adjacent glucopyranose rings define the disaccharide cellobiose unit which appears as a repeated segment along the cellulose structure [11,12].

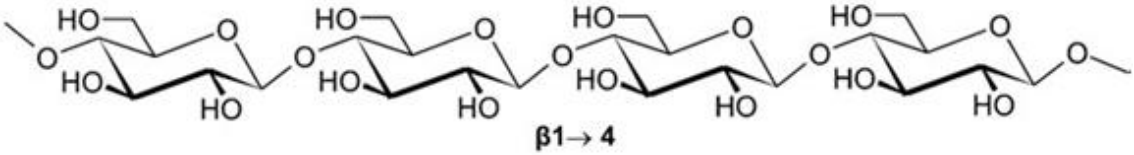

Figure 2 –Cellulose molecular structure.

The cellulose chain length is defined by the number of glucose units (degree of polymerization, DP) [7,12] and depends on cellulose source and isolation process [15]. In the case of native plant cellulose, DP values range between 10,000 for wood cellulose to about 15,000 for cotton cellulose [19]. However, in overall, DP decreases when the cellulose raw materials are subjected to chemical and physical isolation procedures [20].

The molecular structure of this biopolymer is responsible for some of its properties namely hydrophilicity, due to the high density of hydroxyl groups; biodegradability, chain stiffness and broad chemical-modifying capability, through the reactive hydroxyl groups [12,19,21]. Hydroxyl groups are also the basis of the abundant intra- and inter-molecular hydrogen bonds between individual chains that promote their aggregation into cellulose fibers [2,5,7,11,12,22]. In fact, the strong network of hydrogen bonds are responsible for cellulose insolubility in most organic solvents and mechanical strength, among others [12,22].

Cellulose macromolecules aggregation into cellulose fibers creates both ordered and disordered regions (Figure 3) [7,11,12]. Ordered or crystalline regions are characterized by strong hydrogen bonds which allow an almost perfect packing of the cellulose chains [7]. These regions represent about 55-70% of cellulose structure in most plants [11,12,16]. Disordered or amorphous regions, on the other hand, are characterized by cellulose chains further apart making hydroxyl groups available for interactions with other molecules such as water [7].

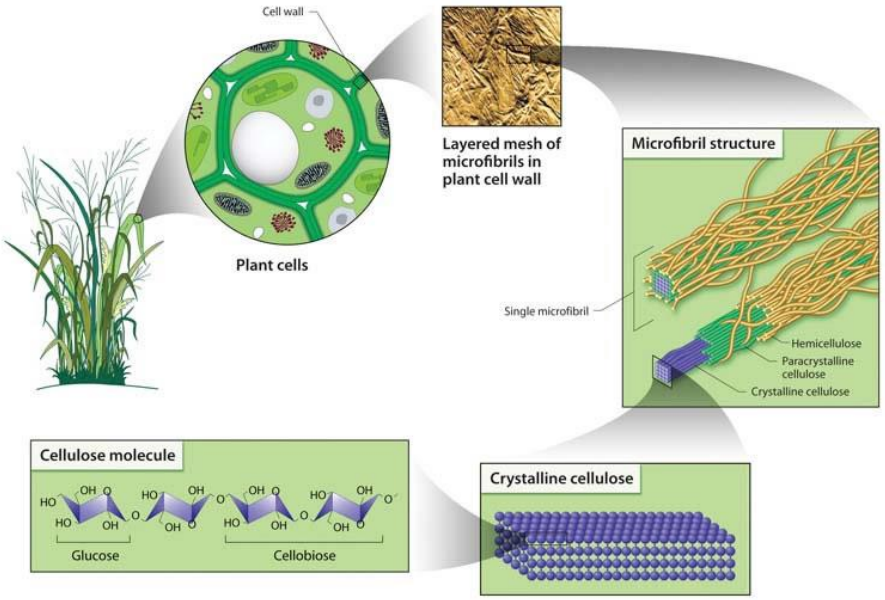

Figure 3 – From the cellulose fiber sources to the cellulose macromolecules [23].

Simultaneous existence of varying order degrees between macromolecules in a fiber enables cellulose to be considered a semicrystalline fibrillar material [11]. In fact, cellulose was the first polymer to be characterized by X-ray diffraction. Through this technique it was revealed that the crystalline structure of native cellulose (cellulose I) can be described by a monoclinic unit cell, which contains two cellulose chains in a parallel orientation (Figure 4). Furthermore, native cellulose was also considered as a mix of two crystalline polymorphs (I_α and I_β), being the I_α/ I_β ratio dependent on cellulose origin. The crystalline structure of these cellulose polymorphs was revealed to have triclinic (I_α) and monoclinic (I_β) unit cells [12].

However, Cellulose I can be converted into other crystal structures (cellulose II, III and IV), among which cellulose II is the most stable form [12].

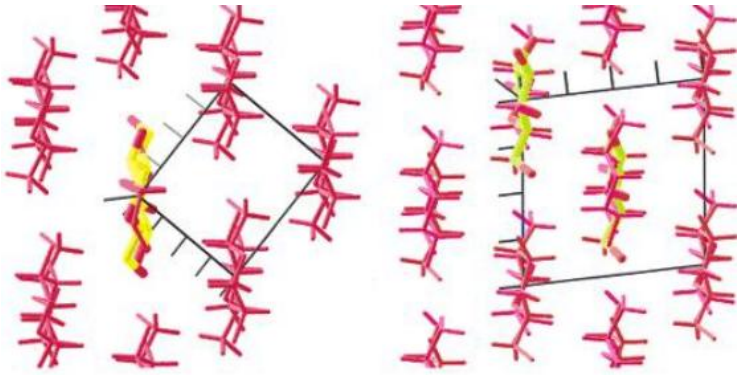

Figure 4 – Crystal structures of cellulose I_α (left) and I_β (right) (reproduced from [24]).

1.3. Bacterial cellulose

Besides plants, cellulose is also produced by some algae (*Valonia*) and bacteria [8–11]. Among these, bacterial cellulose is the one that has attracted more attention, especially due to its ease of production in considerable amounts along with its unique properties [7,12,15].

Bacterial cellulose (also named microbial cellulose) is an extracellular polysaccharide, with the same molecular structure as plant cellulose, produced by several bacteria principally those of the *Gluconacetobacter*, *Sarcina* and *Agrobacterium* genera [12,16,25].

Gluconacetobacter xylinum was the first cellulose-producer bacterium described in literature and until now has been used as a model organism in the study of cellulose biosynthesis and properties. It is a non-pathogenic rod-shaped, obligate aerobic, Gram-negative bacterium capable of producing cellulose from several carbon and nitrogen sources [8,16]. Such bacteria are ubiquitous in Nature, being naturally present wherever the fermentation of sugars takes place, for example, on damaged fruits, and also in unpasteurized juice, beer, and wine [25].

However, *Gluconacetobacter sacchari*, isolated from Kombucha tea, has been recently described by Trovatti *et al.* [26] as an efficient cellulose producer and, therefore, it was employed in the production of the BC membranes used in this study.

1.3.1. Biosynthesis

Bacterial cellulose biosynthesis starts with the production of individual chains (with a degree of polymerization of up to 8000) between the outer and plasma membrane of the bacterial cell, followed by their release outwards through pores on the cell surface. BC chains then assemble into protofibrils, with approximately 2-4 nm of diameter, that further gather into microfibrils of approximately 3-15 nm thick and 70-80 nm wide [12,16,27,28]. Microfibrils, in turn, assemble into a ribbon of crystalline cellulose whose interwoven produces the bacterial cellulose fibrous network [8,9,25], as represented in Figure 5.

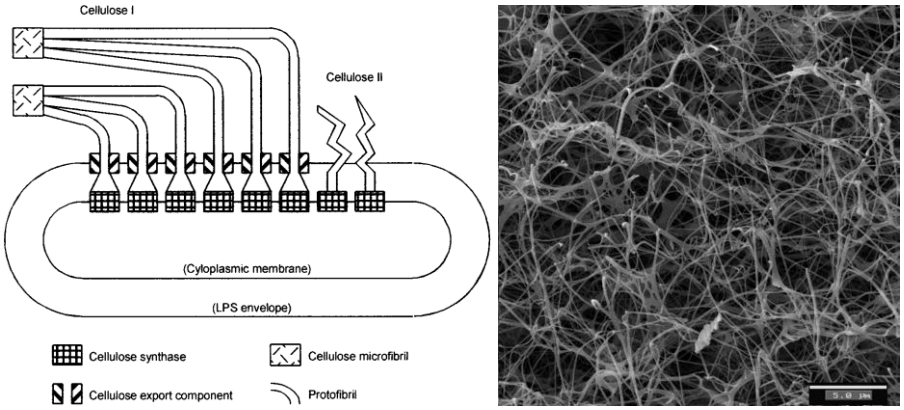

Figure 5 - Schematic illustration of cellulose biosynthesis and fibril formation (reproduced from [29]) and a SEM image of a bacterial cellulose membrane (reproduced from [30]).

BC is produced in standard culture media containing glucose, peptone, yeast extract, citric acid and Na_2HPO_4, after incubation at 30˚C, for several days [26]. Two types of culture method may be used: static and agitated [31–34].

In agitated conditions, BC is synthesized in various forms including fibers, pellets or irregular masses [31,33,34]. It has also been found that some *Gluconacetobacter xylinum* strains, such as JCM 9730 (ATCC 700178), are capable of producing BC as spherical particles [33,34] (Figure 6, left), whose size may be fine-tuned through alteration of the agitation speed applied during culturing [34]. However, the BC produced through this approach exhibits lower degree of polymerization (DP), crystallinity, and Young's modulus than that produced under static conditions. In addition, it has higher water binding ability, possibly due to the higher number of accessible hydroxyl groups in the BC structure associated with its lower crystallinity [31–33,35].

However, the most common method for BC production involves static conditions, from which it is produced as a highly hydrated membrane (Figure 6, right) [25,26] on the air-culture media interface [29,32]. The assembly of such exopolysaccharide has been described as a way to help bacterial cells to remain on the surface of culture medium, where there is high oxygen content; and also offer protection against ultraviolet radiation, natural enemies and drying [12,29].

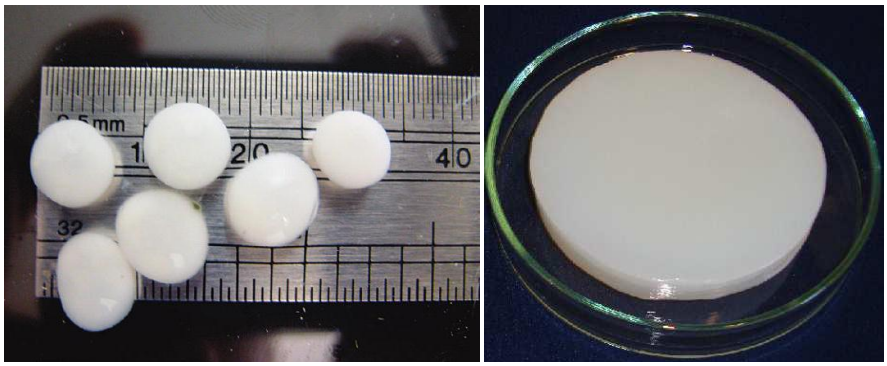

Figure 6 – Photograph of spherical BC particles produced in agitated culture (left) (reproduced from [34]) and a wet bacterial cellulose membrane produced in static conditions (right) (reproduced from [6]) and.

As cellulose is synthesized, a membrane with increasing thickness is generated but, to make that possible, it is assumed that the mature cellulose is constantly pushed down as new cellulose is formed on the surface (Figure 7 left) [27]. Additionally, bacteria are enveloped in their polymerization product and consequently they will also be gradually drawn into deeper zones. The decreased oxygen content in this area promotes bacteria inactivation, but they can be reactivated when placed in their optimum conditions [27].

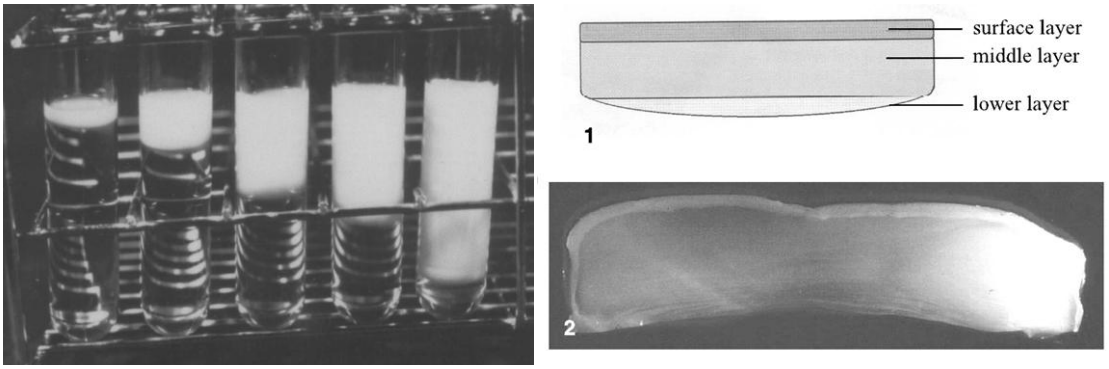

Figure 7 – On the left, bacterial cellulose membranes with different growth times (reproduced from [29]). On the right, (1) schematic representation of cellulose layers in the membrane and (2) cross-section of a purified bacterial cellulose membrane (reproduced from [8]).

As a result, a BC membrane with regions of varying density is generated, namely a dense surface layer, a loose bottom layer and a middle region whose density is intermediate to that of the remaining layers (Figure 7, right) [8,27,28].

Unlike plant cellulose, and despite their molecular similarity, BC is entirely free of hemicelluloses, lignin and pectins [36]. However, after its biosynthesis, some impurities such as bacterial cells and culture medium components remain on the BC membrane [16,22,37]. A treatment with alkaline solutions removes the cells embedded in the cellulose

network and after several washings with pure water the removal of the remaining impurities is achieved [16,26,29], obtaining a high purity biomaterial [8,12,36].

Despite its advantageous properties, BC production is associated with relatively high production costs, due to the use of expensive culture media along with the high time of growth, which may limit the applications of this high value material [15,38]. Therefore, research focus on the use of cheaper carbon and nutrient sources, such as agro-forest industries residues (e.g. grape skin aqueous extract, sulfite pulping liquor and pineapple peel juice) [38–40], as well as the improvement of fermentation efficiency [16] have been conducted.

1.3.2. Properties

As previously described, bacterial cellulose is composed of a network of ribbon-shaped fibrils with average diameter 100 times thinner than that of plant cellulose fibers (Figure 8a,b)[16]. Scanning electron microscopy (SEM) observation of bacterial cellulose revealed the existence of irregular clusters of fibrils in the external surfaces of BC membrane, whereas the transversal SEM images reveal an organization into layers [16]. These fibril layers are piled together through extensive interfibrillar hydrogen bonds (Figure 8c) [8,28,41,42].

In addition, the unique nanostructured morphology of BC results in a highly porous structure both contributing to BC high permeability and high water binding capacity (with a water content of >90%), as compared to cellulose from plants (which have a water content of 60%) [8,12,16,36].

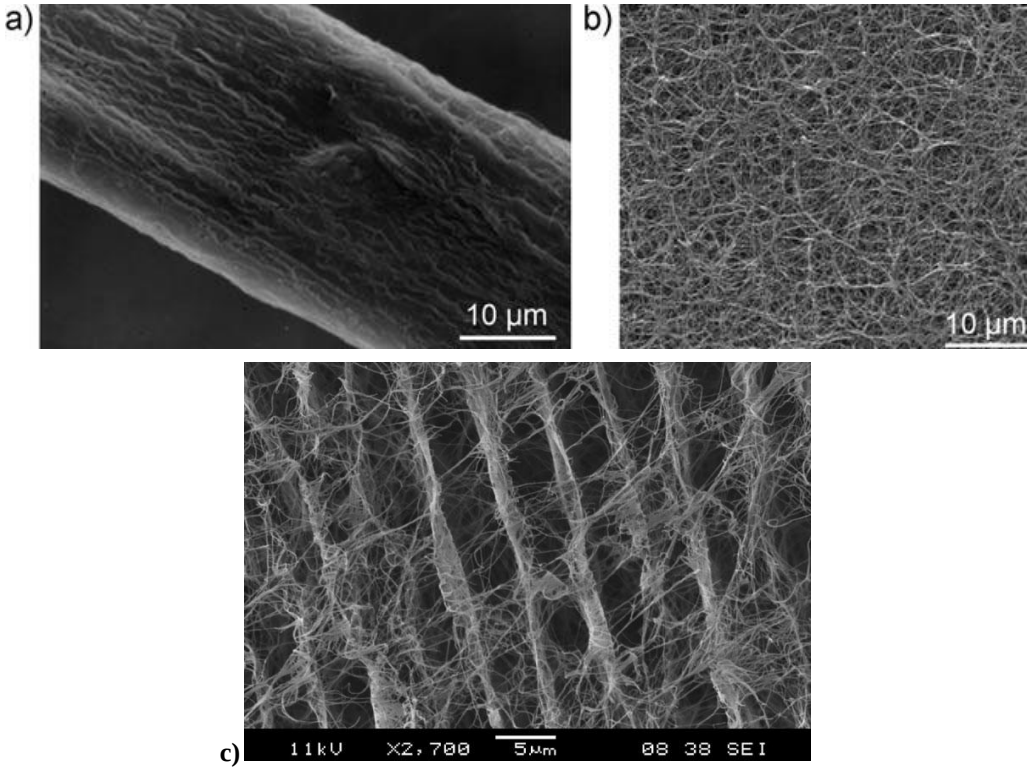

Figure 8 – Scanning electron micrographs of a) plant cellulose fiber, b) bacterial cellulose membrane surface (reproduced from [25]) and c) the cross-section morphology of the BC membrane(reproduced from [43]).

However, upon complete removal of water by air-drying, BC can only reabsorb part of its initial water content because the pore structures collapses and strong hydrogen bonding hinders the membrane to fully rehydrate [44,45]. Nevertheless, when less harsh techniques towards the 3D structure are applied, such as freeze-drying, BC is capable of reabsorbing up to 70% of its initial water content [8,12].

The nanofibers have low density [7] and show a high crystallinity index (60–80%) [12,16,36,37], high mechanical strength with a tensile strength of 200-300 MPa [12,16] and a Young's Modulus of up to 15 GPa [8,12,16,41]; as well as high thermal stability (with a decomposition temperature ranging between 340-370˚C) [46].

The biocompatibility and toxicity of BC has also been accessed, through *in vivo* studies. In these, BC was subcutaneously implanted into rats and the implants were evaluated with respect to any sign of inflammation, foreign body responses and cell viability. The results attained revealed no macroscopic signs of inflammation around the implants and allowed concluding that BC was beneficial to cell attachment and proliferation [47].

The moldability of BC during biosynthesis [48] is another feature that may enable the development of designed shape products [8] directly in the culture media, without subsequent treatment [12], increasing the application range of BC.

1.4. Bacterial cellulose applications

1.4.1. Food

One of the first applications of bacterial cellulose was as raw material for the production of an indigenous dessert in Philippines called nata de coco (Figure 9). It is produced from coconut water fermentation and then cut into pieces and immersed in sugar syrup. Bacterial cellulose is also commercialized in large quantities and exported as a calorie-free and healthy food [12,15,29].

Figure 9 – Nata de coco (reproduced from [49]).

Additionally, bacterial cellulose produced in agitated culture is also employed in the food industry as a thickening agent, texturizer and/or calorie reducer [10,36].

1.4.2. Cosmetics

Bacterial cellulose has also application in the cosmetic industry as facial masks for the treatment of dry skin [50] which are already widely commercialized (Figure 10); in the formulation of natural facial scrub [51], as a structuring agent in personal cleansing compositions [52] and as a stabilizer of emulsions [53].

Figure 10 – Appearance of a cellulose mask after its application onto facial skin (reproduced from [50]).

1.4.3. Biomedical

The unique properties of BC, such as the high water-retention capacity, mechanical strength and biocompatibility; encouraged the development of several products for biomedical applications, especially as wound dressing (Figure 11) [36], temporary skin substitutes [36] and vascular implants [8]. Biofill®, a temporary human skin substitute for second and third degree burns [8], and Nexfill®, a bacterial cellulose dry bandage for burns and wounds [53], are examples of BC products already commercialized.

Figure 11 –A bacterial cellulose dressing applied in wound healing (reproduced from [36]).

The moldability of BC may also be useful in creating specific biomedical products. In fact, such property has already been exploited for the production of a BC membrane in the shape of a glove (as shown in Figure 12, left) [48].

Furthermore, BC potential for application as artificial blood vessels for microsurgery has also been assessed, through its *in situ* biosynthesis into gas permeable tubular molds (Figure 12, right). Results attained are promising since the resulting tube resists to the blood pressure, does not promote any rejection nor inflammation reactions and acts as a scaffold for cell proliferation [8].

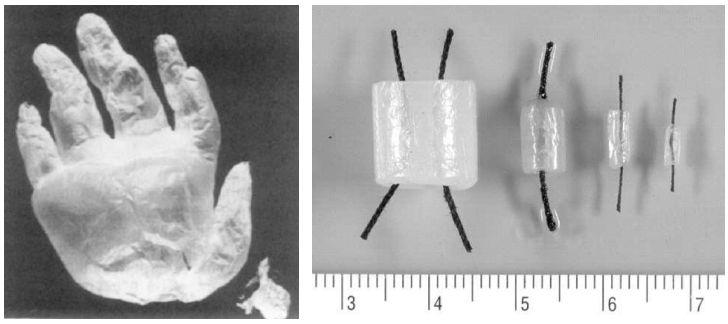

Figure 12 – On the left, bacterial cellulose biosynthesized in the shape of a glove (reproduced from [48]). On the right, bacterial cellulose biosynthesized as tubes with different diameters which can be used for arterial grafting applications (scale bar in cm) (reproduced from [8]).

Bacterial cellulose has also been evaluated as a topical drug release system. Two therapeutically relevant drugs, lidocaine hydrochloride and ibuprofen, were incorporated into wet BC membranes, producing flexible drug loaded membranes with homogenous distribution of the drugs [54,55].

The therapeutic feasibility of such BC membranes in topical and transdermal drug delivery was evaluated through lidocaine and ibuprofen penetration through human epidermis. The results attained for lidocaine (hydrophilic drug) reveal a long-term drug release, possibly resulting from the strong interactions with the BC as well as from a tortuous diffusion pathway along the BC complex tridimensional network, therefore being promising for the treatment of conditions that require a slow drug release.

In the case of ibuprofen (hydrophobic drug), the establishment of weaker interactions with the hydrophilic BC contributes to its rapid released from the BC membrane and therefore it is suitable for the treatment of conditions that require a fast drug release.

Finally, the results attained revealed that BC membranes are a promising drug delivery system having, at the same time, the ability to adhere to irregular skin surfaces, protecting the wound and absorbing exudates [54,55].

1.4.4. Audio membranes

Besides the biomedical applications, bacterial cellulose is also appreciated in a series of technical applications. For instance, SONY Corporation and Ajinomoto developed an audio speaker diaphragm membrane using a compressed low thickness (~20 μm) BC membrane, that is currently utilized in audio headphones (Figure 13).

The application of BC in the development of such products is related to its unique dimensional stability/rigidity and high sonic velocity over a wide frequency range. Additionally, in comparison with conventional diaphragms, based on titanium or aluminum for instance, BC diaphragm produces the same sound velocity along with the warm and delicate sound that the paper diaphragm provides. Trebles are sparkling clear, and bass notes are remarkably deep and rich [7,16].

Figure 13 – Bacterial cellulose diaphragm used in SONY headphones (reproduced from [7]).

1.5. Bacterial cellulose nanocomposites

Besides application of BC membranes in the fields mentioned above, various attempts have been made in order not only to impart BC with new properties, but also to take advantage of BC remarkable properties to improve the performance of existing materials [53,56].

To achieve such goals, researchers have been engaged in the development of BC nanocomposites, produced by (1) introduction of polymers or other components during BC biosynthesis, (2) *in situ* polymerization of different monomers within the BC network, and (3) blending with other polymeric materials (with or without previous chemical modification).

Nanocomposites are materials made from two or more constituents, denominated as matrix and reinforcement, which remain individualized and in which at least one of the reinforcement elements has dimensions less than 100 nm [4,37,56].

The matrix is the continuous phase of the material in which the reinforcement, responsible for imparting the material with specific properties, is embedded. In fact, the main purpose of the development of such materials is the possibility of obtaining products with properties that cannot be attained from the individual constituents [4].

The application of BC nanofibers as reinforcing elements in nanocomposite materials has been one of the emerging areas of interest [25,37] mainly due to their large aspect ratio and high surface area. These properties improve the interaction and adhesion between the fibers and the matrix which in turn contribute for the efficient stress transfer between the two components, and therefore results in composites with improved mechanical properties [4]. In addition, BC nanofibers have a reduced size, smaller than the wavelength of visible-light, disabling them to produce light scattering and making them suitable for the synthesis of transparent materials [8,15,53].

1.5.1. Production of BC nanocomposites during BC biosynthesis

Using this approach BC nanocomposite materials are obtained through the supplementation of culture medium with intended additives. These compounds are incorporated within the BC network during its formation, allowing not only the regulation of the shape and supramolecular structure of cellulose as well as the preparation of composites directly during biosynthesis [25].

For instance, in the study performed by Zhu et al. [57], spherical Fe_3O_4/BC nanocomposites (Figure 14) were produced by supplementation of BC culture medium with Fe_3O_4, under agitated fermentation conditions. Such material has a black color, evidencing the good dispersion of Fe_3O_4 between the BC nanofibrils, and high absorbing ability of heavy metals, like Pb^{2+}, Mn^{2+} and Cr^{3+}. Besides, the paramagnetic character conferred by the Fe_3O_4 allows its easy recovery through the application of a magnetic field. After elution of the adsorbed ions, Fe_3O_4/BC nanocomposites can be reused for further adsorption of the same heavy metal ions [57]. Therefore, this novel nanocomposite has potential as heavy metal adsorbent materials.

Figure 14 – Spherical Fe_3O_4/BC nanocomposites (reproduced from [57]).

Yano *et al.* [58] employed a similar approach for the preparation of BC/silica nanocomposites, through the incorporation of suspensions of silica nanoparticles into the BC culture medium. The ensuing nanocomposites were hot-pressed to produce dry BC/silica nanocomposite films.

The amount of silica loaded in the dry BC-nanocomposites was shown to increase with the amount of silica introduced in the culture medium. However, high concentrations of silica cause a decline in the crystallinity index, the modulus and the tensile strength of the nanocomposite, in comparison with pure BC; possibly caused by the interference of silica nanoparticles in the assembly of cellulose microfibrils into ribbons, as shown in Figure 15.

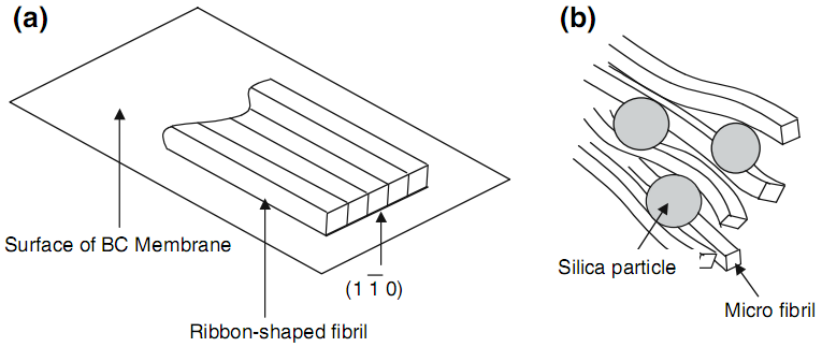

Figure 15 - Deformation of ribbon-shaped fibrils by inclusion of silica nanoparticles into BC culture medium. (A) Ribbon assembly in native BC membrane and (B) disruption of ribbon-shaped fibril formation by silica nanoparticles (reproduced from [58]).

Another example of such approach is the BC/poly(vinyl alcohol) nanocomposite (BC/PVA), obtained through the direct addition of poly(vinyl alcohol) into the culture medium.

SEM analysis of the ensuing nanocomposites reveals that PVA is homogenously dispersed in the BC network and, despite causing a slight increase in the fibrils diameter, PVA incorporation affects neither BC fibrils arrangement nor BC crystalline structure. In addition, the BC/PVA nanocomposites show enhanced transparency, in comparison with the milky-white BC membrane, as well as high strength, stiffness and toughness (Figure 16) [59].

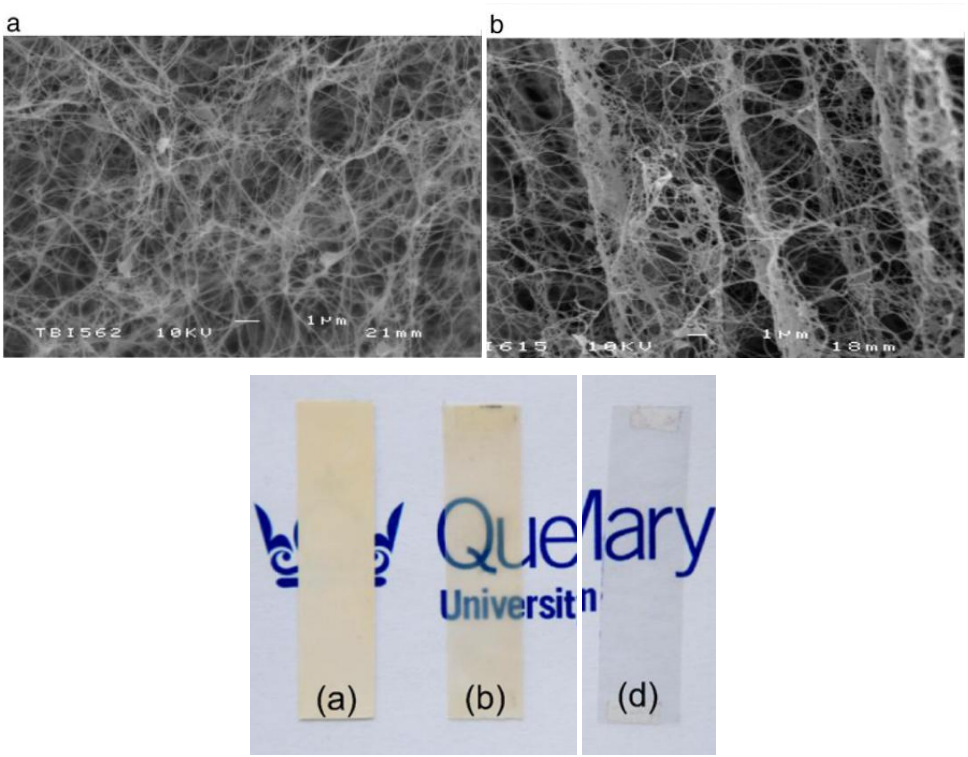

Figure 16 - SEM micrographs of: (a) BC (Magnification 5000), (b) BC/PVA nanocomposite (Magnification 8000) and optical photographs of (a) pure BC, (b) BC/PVA nanocomposite, and (d) pure PVA sheet (reproduced from [59]).

1.5.2. Blending of BC with other polymeric materials

BC nanocomposites may also be prepared by blending with various polymeric matrices, after BC membrane biosynthesis. This can be achieved either by immersion of BC into a polymer solution, allowing the polymer to diffuse into the membrane, or by the addition of BC, in its shredded form, as a reinforcing element of a polymeric matrix/solution [15].

For instance, Cai and Kim [45] impregnated a wet BC membrane with a poly(ethylene glycol) (PEG) solution, followed by freeze-drying. In the resulting material, PEG chains not only penetrated into the BC fiber network but also coated the BC fibrils surface, as verified by fibrils enlargement (Figure 17).

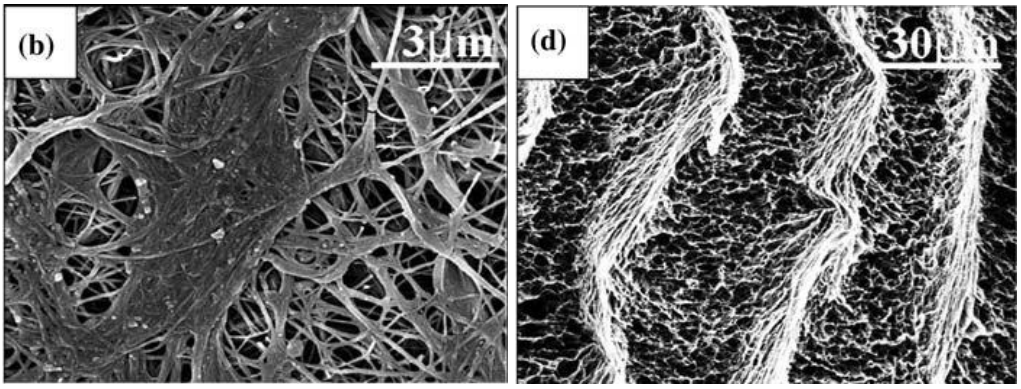

Figure 17 – (b) Surface morphology and (d) c: cross-section morphology of BC/PEG nanocomposite (reproduced from [45]).

The incorporation of PEG into the BC network resulted in a novel material with lower crystallinity than pure BC, possibly a result of the establishment of strong intermolecular interactions between BC and PEG that prevents BC crystallization. This is also the reason for the decreased Young's Modulus and tensile strength of the BC/PEG nanocomposite.

Moreover, the BC/PEG nanocomposite shows increased elongation at break, as a result of the plasticizer effect of the PEG molecules, and better biocompatibility than pure BC, which gives it improved biomedical applications, namely as wound dressing [45].

In another study BC/poly(3-hydroxybutyrate) (PHB) nanocomposites were produced through immersion of BC membranes, previously subjected to solvent exchange from water to chloroform, into a poly(3-hydroxybutyrate) solution in chloroform [60,61].

PHB has attracted attentions in several medical applications so, its combination with BC, may allow its use in tissue engineering area. In fact, introduction of PHB into BC originated the partial filling of porous structure (Figure 18), which may contribute to an effective transfer of nutrients and waste so as to benefit cell growth in the scaffold. Moreover, incorporation of PHB into the BC membranes improves its tensile strength and elongation at break.

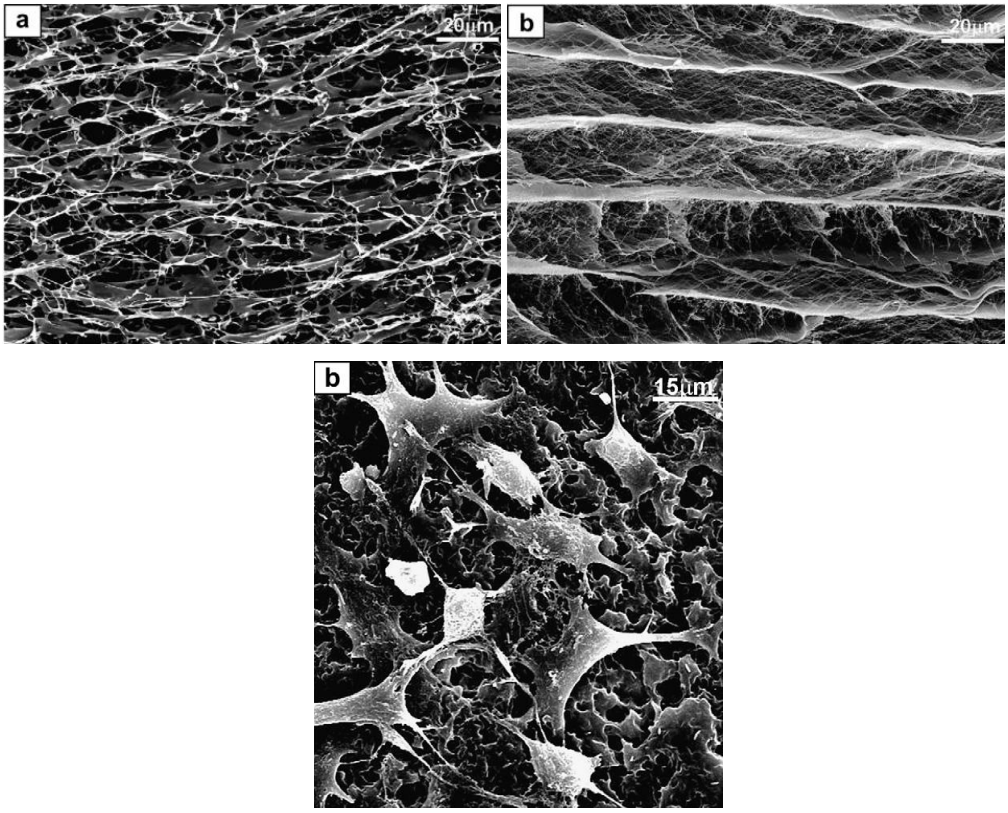

Figure 18 – FESEM images of PHB/BC nanocomposite (a) surface morphology, (b) cross-section morphology, and (down image) Chinese Hamster Lung (CHL) fibroblast cells attachments to PHB/BC nanocomposite scaffold after 48 h seeding the cells (reproduced from [60]).

X-ray diffraction analysis of these nanocomposites was performed in order to evaluate possible alterations in the PHB crystallinity when incorporated into BC. The diffraction pattern of the BC/PHB nanocomposite shows the characteristic peaks of both BC and PHB. However, the peaks of PHB in the PHB/BC nanocomposite were sharper and clearer than those in PHB films. This indicates that the crystallinity of PHB increases with its incorporation into the BC network, possibly because PHB might form crystallites on the surface of the BC nanofibers as they coat them.

Biocompatibility evaluation of the BC/PHB nanocomposite was performed, revealing this novel material to have favorable cell-compatibility in terms of fibroblast cell culture (Figure 18, down image) and better biocompatibility than pure PHB. This way, such material has potential as tissue scaffold namely as an *in vitro* tissue regeneration scaffold [60].

BC has countless interesting characteristics, however it lacks intrinsic antimicrobial properties. So, research activities have been carried out in order to impart this property on BC membranes, through the incorporation of antimicrobial materials such as silver nanoparticles [62,63].

Silver, either in its nanoparticle, metal or ionic forms, is known to exhibit strong cytotoxicity towards a broad range of microorganisms. Incorporation of silver nanoparticles into BC membranes is one of the methods described in literature for the preparation of antimicrobial BC/Ag nanocomposite materials, once their high surface area allows them to produce an effective biocidal action with nanomolar concentrations, in contrast to the micromolar level required with silver ions [62,63].

Two different approaches can be applied: the *in situ* synthesis of the BC/Ag nanocomposites, which involves the impregnation of BC with a silver nitrate ($AgNO_3$) solution followed by Ag^+ reduction [62–64]; and the impregnation of a BC membrane with pre-synthesized Ag nanoparticles [63].

Regardless of the method chosen, the highly porous structure of bacterial cellulose allows Ag nanoparticles to immediately penetrate into it and bound to its microfibrils, probably through electrostatic interactions, generating a yellowish BC membrane (Figure 19) [62,63].

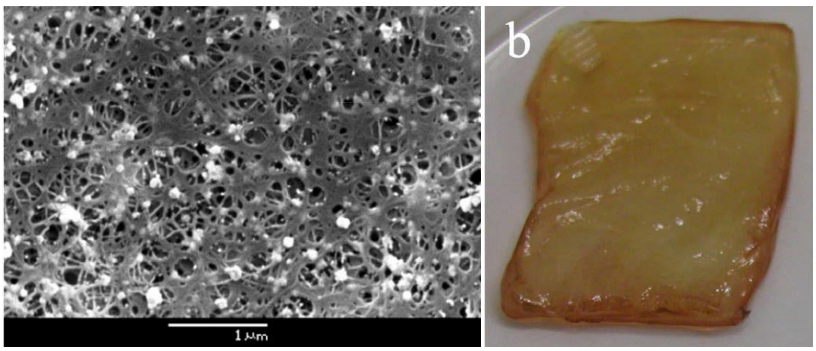

Figure 19 – a) A SEM image of Ag nanoparticles formed into a BC membrane (reproduced from [64]) and b) a wet Ag/BC nanocomposite (reproduced from [63]).

Finally, evaluation of the antibacterial activity of these BC/Ag nanocomposites revealed a complete killing of *Escherichia coli* [62,64], *Staphylococcus aureus* [62–64] and *Klebsiella pneumonia* [63]. Therefore, such material can find potential application as antimicrobial wound dressing, as biofilms for biomedical materials coating or as functional packaging materials [62–64].

Another approach for the preparation of BC nanocomposites makes use of shredded bacterial cellulose. For instance, Martins *et al.* applied this method in the preparation of BC/thermoplastic starch (TPS) nanocomposites through incorporation of BC nanofibers into the TPS matrix during the gelatinization process [65].

This novel material showed good dispersion of the BC nanofibers (Figure 20) as well as a strong adhesion between them and the TPS matrix. Furthermore, addition of low quantities of BC nanofibers increased the tensile strength and Young's modulus as well as the thermal stability of the nanocomposites.

The presence of the BC nanofibers slightly reduces moisture sorption of the BC/TPS nanocomposite. However, this novel material maintains strong sensitivity towards high relative humidity. Therefore, further work would be required to increase its hydrophobic character in order to allow its application as food packaging, for instance [65].

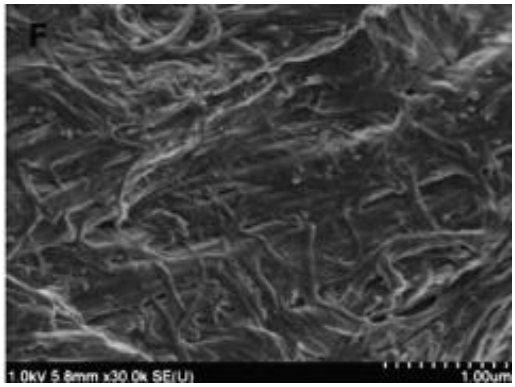

Figure 20 – SEM micrograph of a BC/TPS nanocomposite (reproduced from [65]).

Moreover, a similar approach has been implemented by Tomé, *et al.* [66] in the preparation of composite materials based on poly(lactic acid) (PLA) and BC nanofibers. Due to the hydrophobic character of PLA, a previous acetylation of BC nanofibers was performed in order to improve the compatibility between the two components. SEM analysis of the attained nanocomposites showed a homogenous distribution of the nanofibers into the PLA matrix, revealing the acetylation procedure to be effective in improving the compatibility between BC and PLA.

In addition, the incorporation of acetylated BC nanofibers resulted in increased thermal stability (Figure 21, left) and mechanical properties, as demonstrated by the increments in the initial and maximum degradation temperatures and in both Young's modulus and tensile strength. Moreover, the ensuing material has high transparency (Figure 21, right) and low water sensitivity, making it a good packaging material [66].

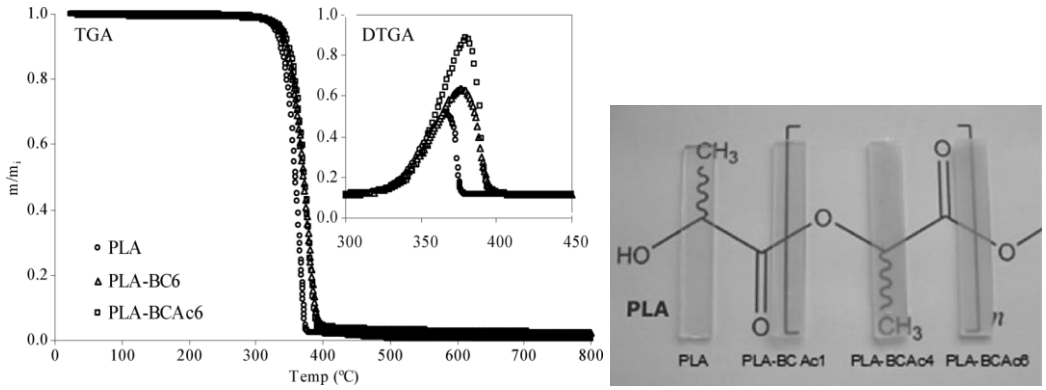

Figure 21 - Thermogravimetric curves of PLA and PLA nanocomposites with 6 wt% of BC (PLA-BC6) and acetylated BC (PLA-BCAc6) (left) and image of the BC/PLA nanocomposite films (right) (reproduced from [66]).

Chitosan, obtained from deacetylation of chitin (the main component of crustacean shells and insects exoskeletons), has numerous properties like biocompatibility and antimicrobial activity [6] which have attracted interest in several fields namely in composite materials synthesis. One of such materials has been prepared by Fernandes *et al.* [67] through the incorporation of BC nanofibers into chitosan matrices.

The structural similarity of chitosan and BC makes them perfectly compatible [6], enabling the preparation of nanocomposite films with homogenous distribution of the BC nanofibers. In addition, the resulting films show high transparency (Figure 22a), flexibility, improved mechanical properties (Figure 22b) and thermal stability [67]. This way, these nanocomposites may be applied as transparent, biodegradable and anti-bacterial packaging materials [67].

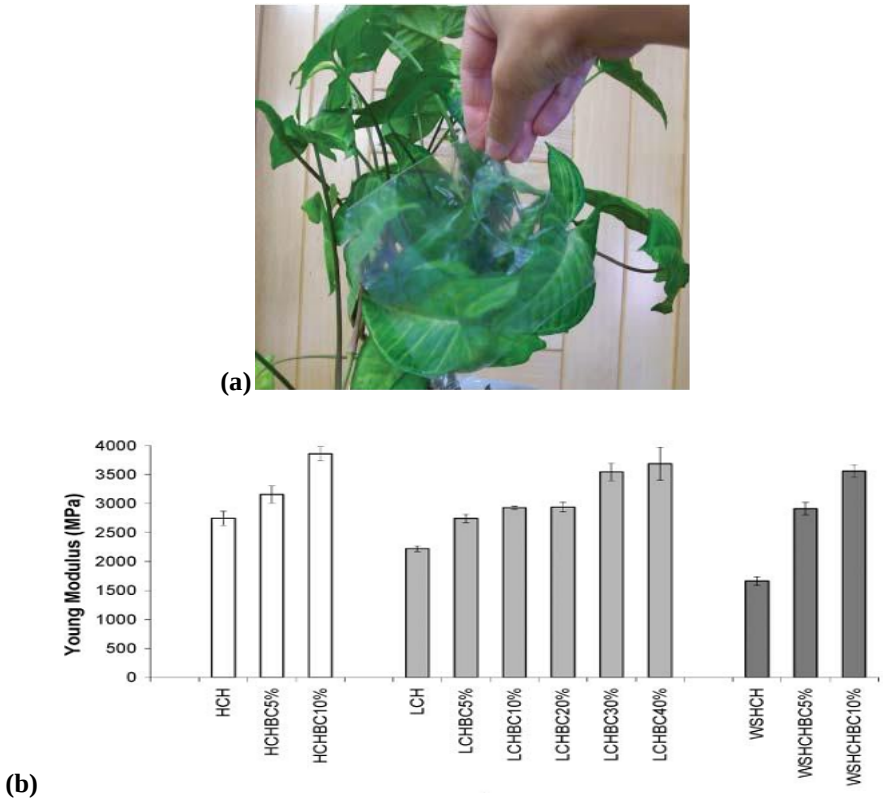

Figure 22 – (a) A transparent BC/chitosan nanocomposite and (b) young's modulus of chitosan samples and their correspondent nanocomposite films with different BC contents (reproduced from [67]).

Other nanocomposite materials have been prepared through casting water-based suspensions of two commercially avaliable acrylic emulsions, composed of random copolymers of butyl acrylate and methyl methacrylate, and bacterial cellulose nanofibrils.

SEM analysis of the resulting nanocomposites revealed good compatibility between the BC and the acrylic matrices. Furthermore, the addition of low amounts of cellulose nanofibers (1-10%) to the acrylic matrices enhanced the mechanical properties as well as the thermal stability (Figure 23) of the final nanocomposites [68].

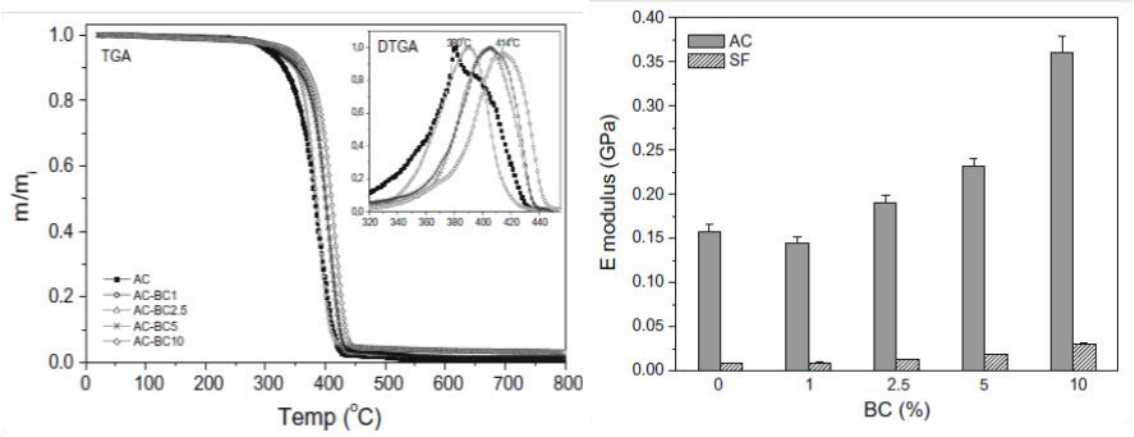

Figure 23 – Thermogravimetric curve of an acrylic copolymer emulsion and the corresponding BC/AC nanocomposites (left) and Young's modulus of the acrylic copolymer emulsions and their corresponding BC-based nanocomposites (right) (reproduced from [68]).

Furthermore, novel pullulan/BC nanocomposite films have also been prepared using this approach [69]. Accordingly, the pullulan matrix was filled with increasing concentrations of BC nanofibers (up to 60% w/w), using glycerol as plasticizer.

The ensuing films are very homogenous, with a good distribution of the nanofibers within the pullulan matrix even at high fiber contents (up to 40% w/w) and are highly translucent (Figure 24a). From the SEM images a complete immersion of the BC nanofibers into the matrix is observed, revealing a strong interfacial adhesion between the two components.

The incorporation of BC nanofibers into the amorphous pullulan matrix is responsible for the increase of the amount of the crystalline part observed for the nanocomposites (Figure 24b), which is further associated to the improvement of the materials mechanical properties. The use of glycerol as plasticizer was shown to increase the flexibility of the films, which is an important property in several applications. Furthermore, the thermal stability of the nanocomposites was also increased, as a function of the BC content. Indeed, the addition of only 5% w/w of BC produced an increment of 3 and 7ºC in the initial and maximum degradation temperatures, respectively (Figure 24c).

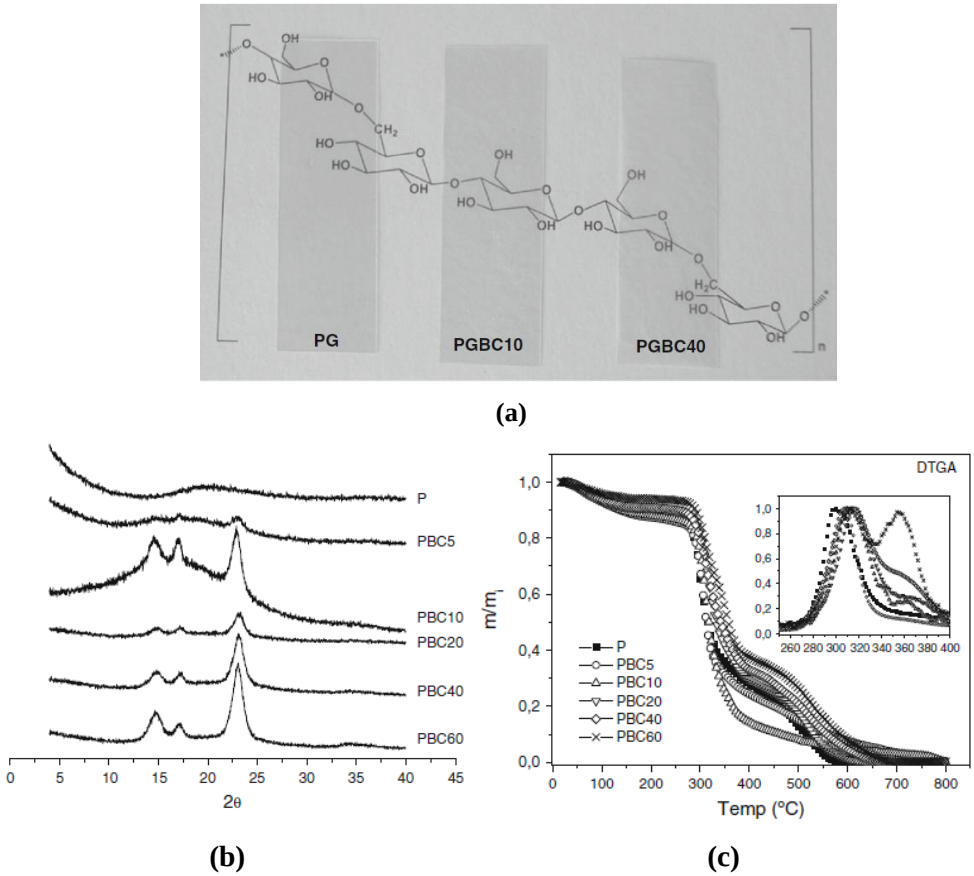

Figure 24 – (a)Visual aspect, (b) X-ray diffractograms and (c) thermogravimetric curves of pullulan and pullulan/BC nanocomposites (reproduced from [69]).

1.5.3. *In situ* polymerization of different monomers within the BC network

Another approach for the preparation of BC nanocomposites is the polymerization of monomers inside the BC network. Such process involves a previous soaking of BC membrane with a solution containing the monomers, eventually including a crosslinker followed by the polymerization step.

For example, BC/polyaniline nanocomposites were prepared by soaking of a wet BC membrane with an aniline solution, and polyaniline was then prepared by the oxidation of aniline [46,70,71]. Polyaniline incorporation into BC generated a dark green membrane, in comparison with the white BC (Figure 25, up). Aniline polymerization was shown to occur on the BC nanofibrils surface, as verified by the increase in their diameter shown in the SEM images (Figure 25, down).

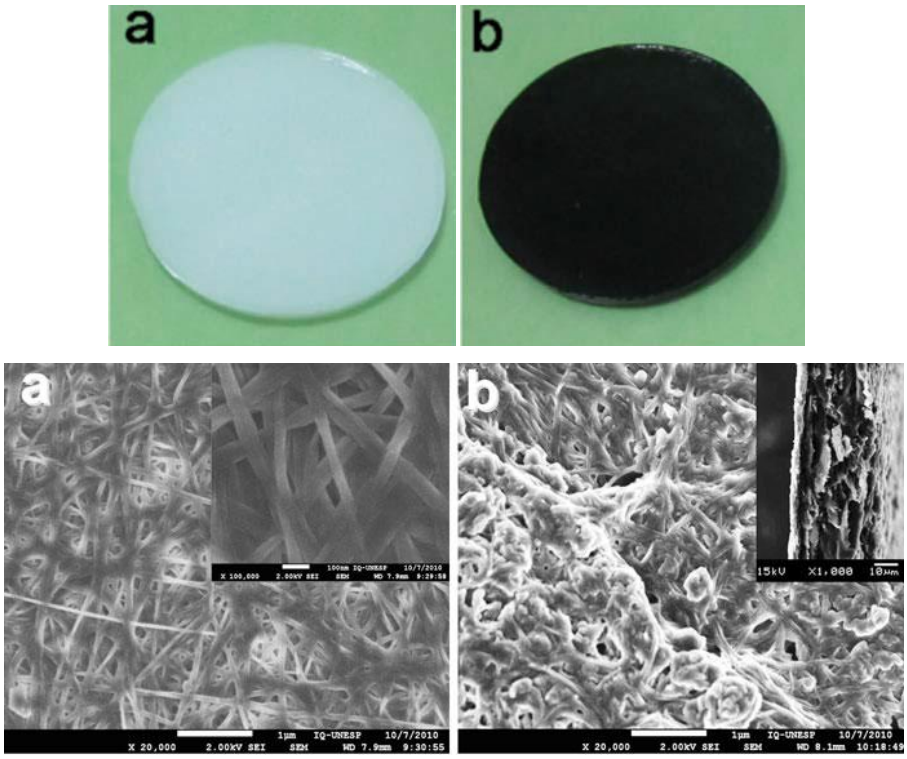

Figure 25 – Up: Photographs of (a) BC hydrogel and (b) BC/polyaniline hydrogel (reproduced from [46]). Down: SEM micrographs of bacterial cellulose (a) and BC/polyaniline hydrogel (b) (reproduced from [70]).

Besides, since polyaniline is a conductive polymer, conductivity analysis of the resulting BC/polyaniline composites was assessed. The attained results showed these materials to be conductive, thereby confirming BC high potential to be used as scaffold for the preparation of conductive materials when combined with conductive polymers, and have potential as optical and electrical displays, biosensors and flexible display devices [46,70,71].

The *in situ* polymerization approach has been also applied in the preparation of BC nanocomposites with various acrylate and methacrylate monomers. For example, BC/methacrylate hydrogels have been prepared by UV radical polymerization of mixtures of the monomers glycerol methacrylate (GMMA) [72], 2-hydroxyethyl methacrylate (HEMA) [72,73], 2-ethoxyethyl methacrylate (EOEMA) [72], 2-ethylhexyl acrylate (EHA) [73] and N-vinyl pyrrolidone (NVP) [73], previously incorporated into BC. All the monomers were polymerized in aqueous conditions, except the hydrophobic EOEMA and EHA monomers which required a solvent exchange in the BC membrane, from water to 2-propanol and ethanol, respectively, to increase the compatibility between the components and allow the diffusion of the monomer into the membrane prior to the polymerization step.

All nanocomposites showed good distribution of the polymers throughout the BC network [72] and, when only the crosslinker content was changed (from 30 to 60 wt%), it was shown that at higher crosslinker concentrations an almost total filling of the BC porous structure is achieved, in comparison with the partial cover of the fibers when using lower crosslinker concentrations (Figure 26a) [73].

The water-swelling ability of the nanocomposites was also investigated and showed to be dependent on the type of monomer and also on the crosslinker concentration employed (an example of a swollen nanocomposite is shown in Figure 26b). Obviously, hydrophilic monomers allowed higher water adsorption than the hydrophobic ones [72,73]. However, this problem can be overcome through combination of hydrophilic and hydrophobic monomers. Furthermore, higher concentrations of crosslinker produced a decrease in the swelling ability, due to the almost complete BC network filling [73].

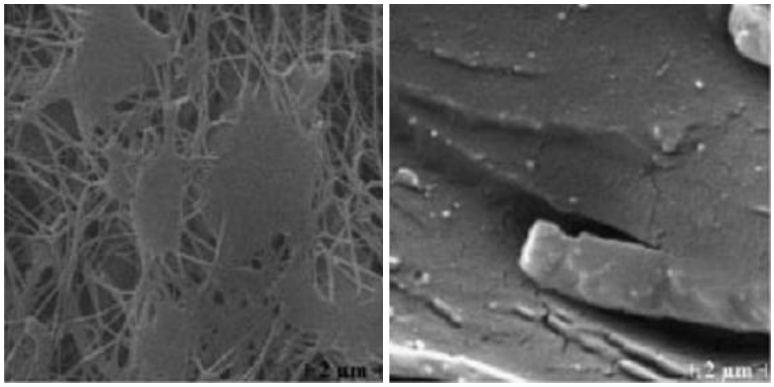

(a)

(b)

Figure 26 – (a) SEM images of freeze-dried BC/polymer nanocomposite with 30 wt% (left) and 60 wt% (right) crosslinker (reproduced from [73]) and (b) Photograph of the BC–poly(HEMA-*co*-EOEMA) composite in the swollen state (reproduced from [72]).

Finally, the mechanical properties of the acrylic gels were improved as a result of BC reinforcement. This way, considering the biocompatibility and non-toxicity of

bacterial cellulose as well as the wide biomedical applications of methacrylate monomers-based materials, such BC-hydrogel composites may have application in tissue engineering namely as a soft tissue replacement (e.g. cartilage) [72,73].

A series of BC/poly(2-hydroxyethyl methacrylate) (BC/PHEMA) nanocomposites were also prepared through the *in situ* polymerization of 2-hydroxyethyl methacrylate monomer (HEMA) [74]. Variable amounts of HEMA and poly(ethylene glycol) diacrylate (PEGDA) as crosslinker were used and impregnated into the BC membranes prior to the polymerization step.

The amount of polymer incorporated into BC increased with the amount of HEMA added as well as with the amount of crosslinker (PEGDA), and a homogenous distribution of PHEMA in the BC network was observed.

PHEMA incorporation into the BC membrane produced nanocomposite films more translucent than pure BC and with improved thermal stability than pristine PHEMA matrices (Figure 27, left). The increasing PHEMA content resulted in decreased crystallinity and mechanical properties. In addition, the nanocomposite films showed increased swelling ability, in comparison with BC membranes, associated with the hydrophilic character of PHEMA and to its ability to prevent the collapse of BC nanostructure during drying.

Finally, biocompatibility studies (Figure 27, right) showed BC/PHEMA nanocomposites to be non-citotoxic and to favor adhesion and proliferation of human adipocite-derived stem cells (ADSCs) [74]

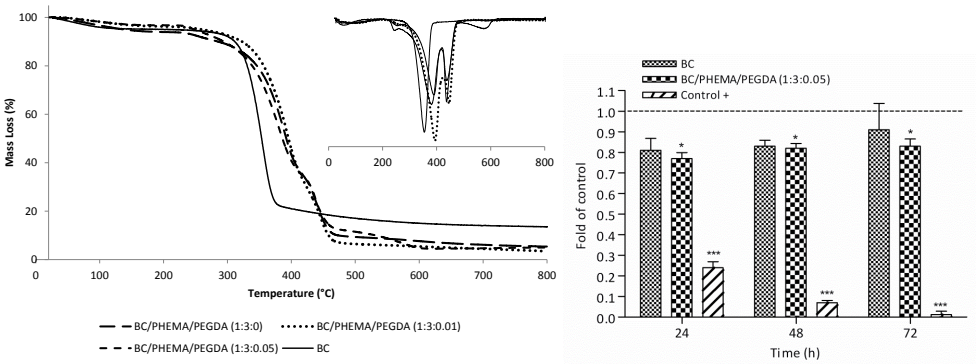

Figure 27 – Left: TGA thermograms of BC/PHEMA/PEGDA (1:3:0), BC/PHEMA/PEGDA (1:3:0.01) and BC/PHEMA/PEGDA (1:3:0.05). Right: ADSCs proliferation on contact with BC, BC/PHEMA/PEGDA (1:3:0.05) membranes, and positive control (polyvinyl chloride, PVC) during 24, 48 and 72 hours (reproduced from [74]).

Besides the *in situ* polymerization, atom transfer radical polymerization (ATRP) was also shown to be suitable method for the modification of bacterial cellulose membrane. Lacerda *et al.* employed this approach in the preparation of bacterial cellulose grafted with either methyl methacrylate (BC-*g*-PMMA) or *n*-butyl acrylate (BC-*g*-BA). The preparation of these nanocomposites required a two steps procedure: first the immobilization of the ATRP initiator followed by the grafting of MMA or PBA from the bacterial cellulose macroinitiator [75].

The attained nanocomposite materials were white opaque, in contrast with the translucid milky-white BC (Figure 28A).

In overall, the properties of the nanocomposites prepared depend on the amount of polymer grafted into the BC membrane. Materials with high polymer incorporation have TGA profiles similar to that of the corresponding homopolymer, while for materials with lower polymer incorporation it resembles more the TGA profile of BC. This behaviour is also seen in the X-ray diffractograms, with the diffraction peaks of cellulose appearing more evident in the material with lower polymer grafted.

Furthermore, grafting of PMMA or PBA conferred BC membranes a high hydrophobic character, as indicated by water contact angles of 134° for BC-g-PMMA and 116° BC-g- BA nanocomposites in contrast with the BC water contact angle of 32º (Figure 28B).

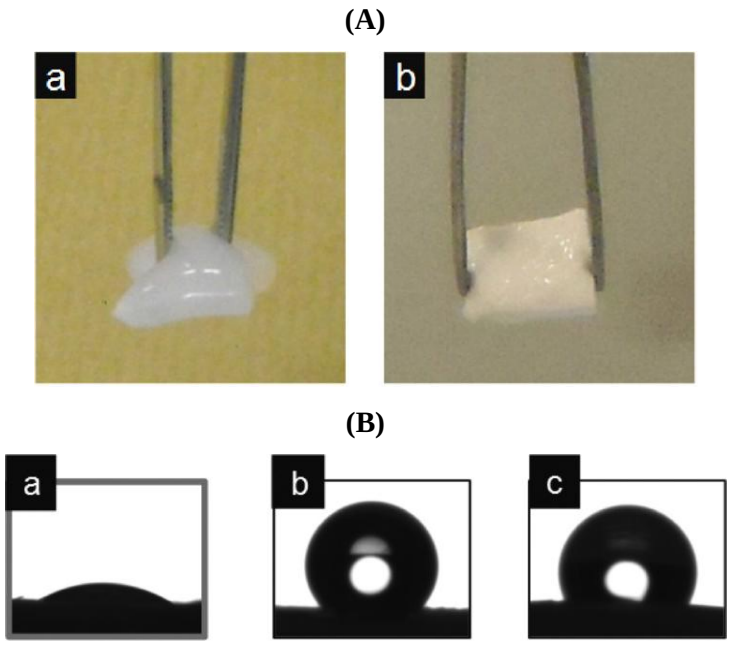

Figure 28 – (A) Photographs of (a) pristine bacterial cellulose and (b)BC-g-PMMA wet membranes. (B) Contact angle pictures of water droplet over (a) pristine BC, (b) BC-g-PMMA, and (c) BC-g-PBA. (reproduced from [75]).

Grafted nanocomposites BC-g-PMMA and BC-g-PBA also show decreased mechanical properties as a result of the higher flexibility of the acrylate polymers than the BC nanofibrillar network.

Finally, the covalent link established between BC and the synthetic grafts prevents leaching during use, allowing the overcome of common limitation of many composites.

1.6. Poly(2-Aminoethyl Methacrylate)

2-Aminoethyl methacrylate hydrochloride (AEM) (Figure 29, left) is a commercially available, water soluble, primary amine-based methacrylic monomer, prepared by the reaction of methacryloyl chloride with 2-aminoethanol hydrochloride at 95ºC [76,77].

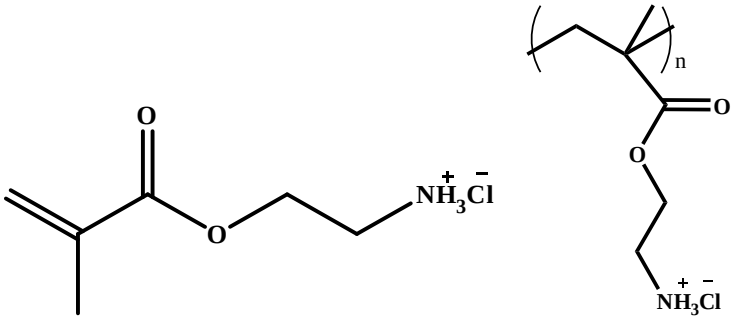

Figure 29 - 2-Aminoethyl methacrylate (AEM) as a hydrochloride salt (left) and its corresponding polymer (right).

AEM monomer has a pK_a near 8.8 and is unstable in alkaline media (pH>9). At this pH the amine groups are on their free form and undergo internal rearrangement into the thermodynamically more stable isomer, 2-hydroxyethyl methacrylamide. However, when in its hydrochloride form as well as in acidic or neutral media, AEM is indefinitely stable [78].

From the radical homopolymerization of AEM it is possible to obtain poly(2-aminoethyl methacrylate) (PAEM) (pK_a≈7.6) (Figure 29, right) [76,77], whose preparation and application has been described in various studies.

For example, Ji, *et al.* investigated the potential of PAEM vesicles for DNA vaccine delivery [79]. It can also be used as potential vesicles for drug delivery through the preparation of copolymers of AEM and poly(γ-2-chloroethyl-L-glutamate) (PCELG) [80]. Such copolymers may also be pH-temperature responsive, as in the particular case of AEM and *2*-hydroxypropyl acrylate copolymer described by Deng, *et al* [81]. This way, they can be applied not only as a drug carrier but its action may be controlled by pH and temperature stimuli.

PAEM has also been applied in the development of novel materials, through its blending with carboxymethyl cellulose [82] and sodium alginate [83], as well as protein-resistant coatings, prepared by copolymerization of AEM with either poly(ethylene glycol) methyl ether methacrylate (PEG) [84] or 2-carboxyethyl acrylate (CEA) [85].

Additionally, the polycationic nature of PAEM is responsible for its antimicrobial properties [84], being more active against Gram-positive bacteria as compared to Gram-negative [79]. In fact, polymers with pendant ammonium groups are known to be effective against a broad spectrum of micro-organisms. The mechanism by which PAEM and similar compounds kill bacteria has been related to interaction of their positively charged groups with the negatively charged bacterial cells. From this results the disruption of the cytoplasmatic membrane, leakage of intracellular components and, ultimately, cell death [84,86,87].

Following on what has been described above, the present work aims at imparting antimicrobial properties into BC membranes, through the *in situ* radical polymerization of 2-aminoethyl methacrylate (AEM) inside the BC network. In order to promote the retention of the polymer inside the membrane *N,N*-methylenebis(acrylamide) (MBA) was used as crosslinker. The obtained materials will be characterized in terms of their structure, morphology, thermal stability, mechanical properties and antibacterial activity.

2. Experimental procedure

2.1. Materials

2-Aminoethyl methacrylate in its hydrochloride form (AEM) (Sigma-Aldrich), *N*,*N*-methylenebis(acrylamide) (MBA) (Sigma-Aldrich) and 2,2-Azobis(2-methylpropionamidine) dihydrochloride (ABMPA) (Sigma-Aldrich) were used as received. All other solvents and reagents were of analytical grade and also used as received.

Bacterial cellulose (tridimensional network of nano and microfibrils with 10–200 nm width) in the form of wet membranes was produced in our laboratory using the bacteria *Gluconacetobacter sacchari* and conventional culture medium conditions [26].

2.2. Preparation of neat poly(2-aminoethyl methacrylate hydrochloride) without (PAEM) and with crosslinker (PAEM/MBA).

For the preparation of neat PAEM polymer a solution of 500 mg of AEM and ABMPA initiator (1% *w/w* AEM) in 10 ml of water was prepared in Erlenmeyers stopped with rubber septa. The solution was then purged with nitrogen and placed at 70ºC for 6 hours. The preparation of PAEM/MBA was conducted in the same manner as for PAEM, with the addition of 20% ($w_{crosslinker}/w_{monomer}$) MBA crosslinker to the monomer and initiator solution.

For the purification of PAEM/MBA, the material was washed several times in water and then freeze-dried. In the case of PAEM this strategy couldn't be adopted due to its high water solubility. Therefore, PAEM purification was attempted through precipitation and dialysis and confirmed through CP-MAS ^{13}C NMR. The comparison of the spectra of PAEM precipitated and dialyzed revealed no differences and therefore the PAEM characterized throughout this study was obtained through freeze-drying.

2.3. Preparation of bacterial cellulose (BC)/PAEM nanocomposites

Wet BC membranes (~100 mg, 4×4 cm) were weighted and 60% of its water content was removed with adsorbent paper. Drained BC membranes were placed in Erlenmeyers stopped with rubber septa and purged with N_2. At the same time, aqueous solutions containing both the monomer AEM and the initiator ABMPA (1% *w/w*) were prepared and also purged with nitrogen (in an ice bath) for 30 minutes. When the crosslinker was used, 20% ($w_{crosslinker}/w_{monomer}$) was added to the solution. Thereafter, the aqueous solution was added, with the aid of a syringe, to the Erlenmeyers containing the

BC membranes and they were left to stand for 1 hour at room temperature (25ºC) until the complete absorption of the solution. The reaction mixtures were then placed at 70ºC for 6h. After that period, the septum was removed and the composite membranes were washed with water (100 ml) during 1 hour. This procedure was repeated eight times. The washed membranes were placed over Petri dishes and dried at 40 °C overnight. The dried membranes were kept in a desiccator until their use.

The mechanical analysis of BC, BC/PAEM and BC/PAEM/MBA required BC membranes with 6*6 cm that were prepared using the same procedure previously described for 4*4 cm membranes. The increase of the membrane size was required once the 4 cm long specimens were not enough to have a 3 cm long test area required in such analysis.

2.4. Characterization Methods

CPMAS ^{13}C NMR spectra were recorded on a Bruker Avance III 400 spectrometer operating at a B0 field of 9.4 T using 9 kHz MAS with proton 90° pulse of 3 microseconds and a time between scans of 3 seconds. ^{13}C CPMAS NMR spectra were acquired using a contact time of 2000 (2000) microseconds. ^{13}C chemical shifts were referenced with respect to glycine (C=O at 176.03 ppm).

FTIR spectra were acquired using a Perkin Elmer FT-IR System Spectrum BX spectrophotometer equipped with a single horizontal Golden Gate ATR cell. Thirty-two scans were acquired in the 4000−500 cm^{-1} range with a resolution of 4 cm^{-1}.

Thermogravimetric analyses (TGA) were carried out using a Shimadzu TGA 50 analyser equipped with a platinum cell. Samples were heated at a constant rate of 10 °C/min, from room temperature to 800 °C, under a nitrogen flow of 20 mL/min.

Tensile tests were performed on a tensile testing machine (Instron 5564) at a cross-head speed of 10 mm/min using a 1 kN static load cell. The tensile test specimens were rectangular strips (30 mm×10 mm) dried at 40ºC and equilibrated in a 50% humidity atmosphere prior to testing. All measurements were performed for at least three replicates for each case and the average value was recorded.

SEM micrographs of the nanocomposite film surfaces were obtained on a HR-FESEM SU-70 Hitachi equipment operating at 1.5 kV and that of BC was taken with a Hitachi S4100 equipment operating in the field emission mode. Samples were deposited on a steel plate and coated with carbon before SEM observation.

The X-ray diffraction (XRD) measurements were carried out with a Phillips X'pert MPD diffractometer using Cu Kα radiation.

The swelling ratio (SR) of the nanocomposite films was measured using the weighing method [5]. Specimens (dimensions 1 x 1 cm) were immersed in distilled water at room temperature to study their swelling, with a minimum of three replicates (tested for each material). The weight increase was periodically assessed for 48 hours. Samples were taken out of the water, their wet surfaces immediately wiped dry in filter paper and then re-immersed. Then the SR was calculated using the equation below:

$$SR(\%) = \frac{(Ws - Wd)}{Wd} \times 100\%$$

where W_d is the initial weigh of dry film and W_s is the weight of the film swollen in water.

2.5. Assessment of BC nanocomposites antimicrobial properties

2.5.1. Bacterial strain and growth conditions

The antimicrobial activity of the BC/PAEM nanocomposites was tested against the recombinant bioluminescent strain of *Escherichia coli*, containing two plasmids that confer resistance to two antibiotics: ampicilin (Amp) and chloramphenicol (Cm) [88]. Stock cultures were stored at -80ºC in 10% glycerol.

Before each assay, an aliquot of *E. coli* was aseptically plated on tryptic soy agar (TSA, Merck) supplemented with 100 mg mL-1 of Amp and 25 mg mL-1 of Cm and grown for one day at 25 °C. Next, one colony was aseptically inoculated on tryptic soy broth (TSB, Merck) with both antibiotics and grown for one day at 25 °C under stirring (120 rpm). Then, an aliquot of this culture was subcultured in 30 mL of TSB with Amp and Cm and grown overnight at 25 °C under stirring (120 rpm).

To assess the antimicrobial activity of the BC/PAEM nanocomposites ~50 mg of each material was placed in contact with a bacterial liquid suspension, prepared by

tenfold diluting an overnight grown bacterial culture in TSB. Control bacterial cellulose samples were also run in each antibacterial test and all samples were incubated at 25ºC. At time 0 and after 1, 2, 4, 6, 9, 12, 24 hours of contact an aliquot of each sample and control was collected and the bioluminescence was measured in the luminometer (TD-20/20 Luminometer, Turner Designs, Inc., USA). This experiment was done in triplicate and the results were averaged.

2.5.2. Bioluminescence versus CFU

To evaluate the correlation between the CFU and the bioluminescence signal of *E. coli* an overnight culture of bioluminescent *E. coli* was serially diluted (10^{-1} - 10^{-7}) in fresh phosphate buffered saline (PBS) 1x (8 g/L NaCl, 0.2 g/L KCl, 1.44 g/L Na_2HPO_4 and 0.24 g/L KH_2PO_4; pH 7.4). Non-diluted and diluted aliquots were pour plated on TSA medium (1 mL) and, simultaneously, were read on a luminometer (500 μL) (TD-20/20 Luminometer, Turner Designs, Inc., USA) to determine the bioluminescence signal (measured in relative light units – RLU). This experiment was done in triplicate and the results were averaged.

3. Results and discussion

The present study began with some optimization steps, in order to achieve the best monomer and crosslinker amounts to be used in the nanocomposites preparation (the results are summarized in Table 1). From all the optimizations performed, the approach chosen for the preparation and characterization of the BC/PAEM nanocomposite materials has BC/PAEM ratio of 1:6 and a 20% ($w_{crosslinker}/w_{monomer}$) MBA content.

Table 1 - Identification of the nanocomposite films and its component contents estimation that lead to the method optimization.

BC/PAEM nanocomposites	**BC size (cm)**	**m(AEM) (g)**	**%PAEM**	**%BC**
BC:PAEM (1:5)	2*2	0.26	75.7	24.3
BC/PAEM (1:2)	2*2	0.035	26.7	73.3
BC/PAEM/PEGDA (1:2:0.05)			24.6	75.4
BC/PAEM/PEGDA (1:2:0.20)			27.4	72.6
BC/PAEM/MBA (1:2:0.05)			20.5	79.5
BC/PAEM/MBA (1:2:0.20)			34.7	65.3
BC/PAEM/MBA (1:6:0)	2*2	0.25	69.2	30.8
BC/PAEM/MBA (1:6:0.20)			82.7	17.3
BC/PAEM/MBA (1:6:0)	4*4	0.70	66.9	33.1
BC/PAEM/MBA (1:6:0.20)			85.7	14.3

BC/PAEM nanocomposites without and with 20% (*w/w*) crosslinker (MBA) were prepared by conventional radical polymerization in drained BC membranes previously soaked with an AEM solution. The schematic representation of PAEM polymerization/crosslinking reaction is shown in Figure 30.

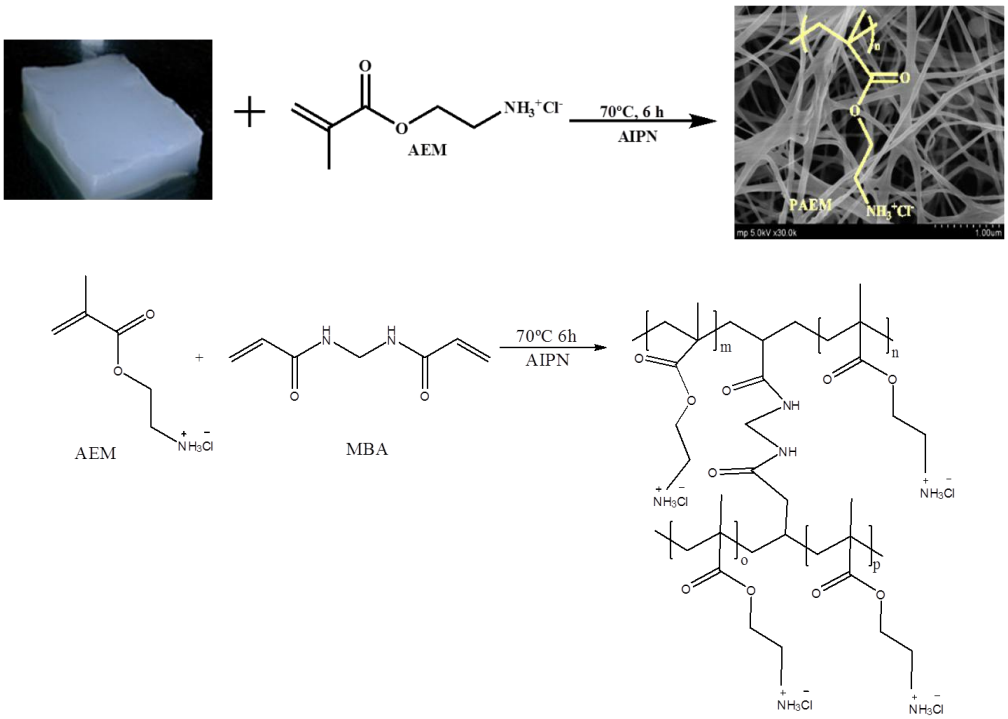

Figure 30 – Schematic representation of the 2-aminoethyl methacrylate hydrochloride (AEM) polymerization into poly(2-aminoethyl methacrylate) (PAEM), inside the BC network. As well as the schematic representation of the AEM polymerization, in the presence of MBA, to yield PAEM cross-linked with MBA.

The purified, wet BC/PAEM and BC/PAEM/MBA nanocomposite membranes show a yellowish colour, in comparison with the milky-white BC membrane (Figure 31a). In addition, the BC/PAEM material is malleable, like BC, while BC/PAEM/MBA is tough and very difficult to remove from the Erlenmeyer where the polymerization reaction took place.

After air-drying, all nanocomposite films were visually very homogeneous, with a yellowish colour and considerably more translucent than the pristine BC membrane (Figure 31b).

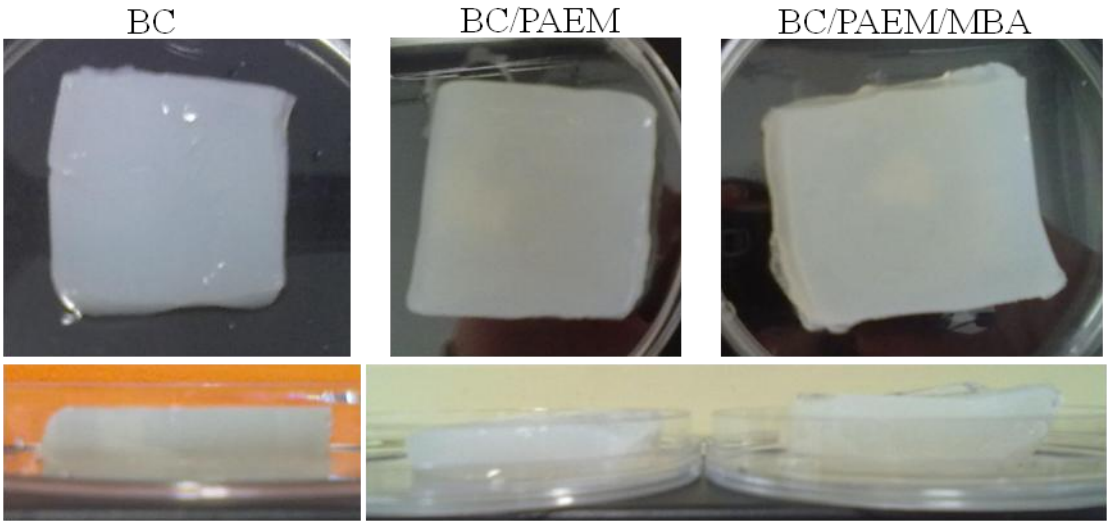

(a)

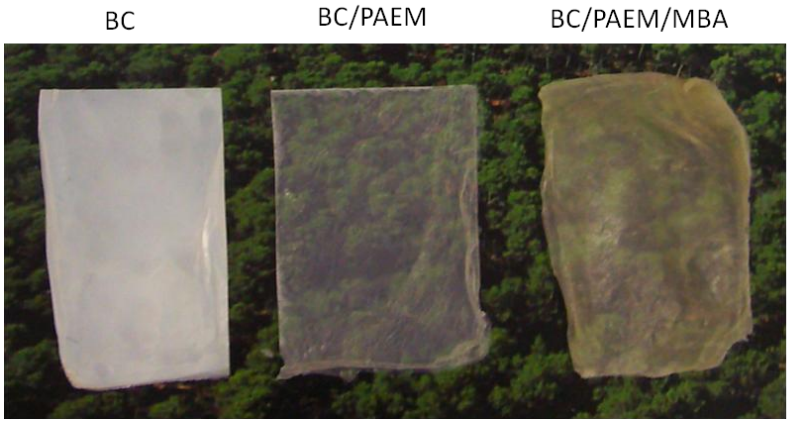

(b)

Figure 31 - Visual aspect of the (a) wet and (b) dry BC, BC/PAEM and BC/PAEM/MBA nanocomposites.

The use of MBA as crosslinker allowed a higher retention of polymer into the BC membrane, as observed by the stronger yellow colour of the BC/PAEM/MBA membranes in comparison with BC/PAEM counterparts (Figure 31). This is further confirmed by the gravimetric measurements (Table 2) and is ascribed to the crosslinking reaction which hinders PAEM removal from the BC network during washings steps, or later in any application of the material.

Table 2 – Identification of the nanocomposite films, its dry weight and its component contents.

BC/PAEM/MBA Nanocomposites	BC membrane size (cm)	Dry BC (mg)	AEM (g)	MBA (%)	Dry material (g)	PAEM[a] %	BC[a] %
BC/PAEM (1:6)	4*4	100	0.70	0	0.38	60.9	39.1
BC/PAEM/MBA (1:6:0.20)				20	0.95	85.2[b]	14.8
BC/PAEM (1:6)	6*6	350	2.0	0	0.97	62.5	37.5
BC/PAEM/MBA (1:6:0.20)				20	2.6	86.4[b]	13.6

[a] PAEM and BC percent composition of the nanocomposites were estimated based on the mass difference between the nanocomposites and BC.

[b] The polymer content values in the case of crosslinked nanocomposites represent not the PAEM but the PAEM/MBA content in the material.

3.1. Structural characterization of the BC/PAEM nanocomposites

The success of the polymerization of AEM into the BC network, either in the presence or absence of MBA, was assessed through FTIR-ATR and ^{13}C NMR analysis.

3.1.1. FTIR-ATR characterization

The FTIR spectra of BC, PAEM, PAEM/MBA and BC/PAEM (with and without crosslinker) are shown in figure 32.

The FTIR spectrum of pure BC is characterized by a broad band at 3500-3000 cm^{-1}, attributed to O–H stretching vibrations; at 2892 cm^{-1} associated with C–H stretching vibration of CH_2 groups, and a sharp and steep band at around 1100 cm^{-1} due to the presence of C–O-C stretching vibration of the ether linkage of cellulose [61,89–91].

The main bands observed for PAEM can be assigned to the amine N-H stretching (3380 cm^{-1}), C-H stretching from CH_2 and CH_3 groups (3300-2500 cm^{-1}), carbonyl ester group stretching (1717 cm^{-1}), N-H bending (1602 cm^{-1}), C-H asymmetrical bending from CH_3 and CH_2 groups (1457 cm^{-1}), C-H symmetrical bending from CH_3 groups (1380 cm^{-1}), CH_2 twisting and wagging (1267 cm^{-1}), ester C-O-C stretching overlapped with C-N stretching (1134 cm^{-1}), CH_3 rocking (970 cm^{-1}) and characteristic CH_2 rocking of the methacrylic polymers (746 cm^{-1}).

The FTIR spectrum of PAEM/MBA shows a similar profile to that of PAEM, once the new vibrations resulting from MBA are overlapped with those already present in the PAEM spectrum.

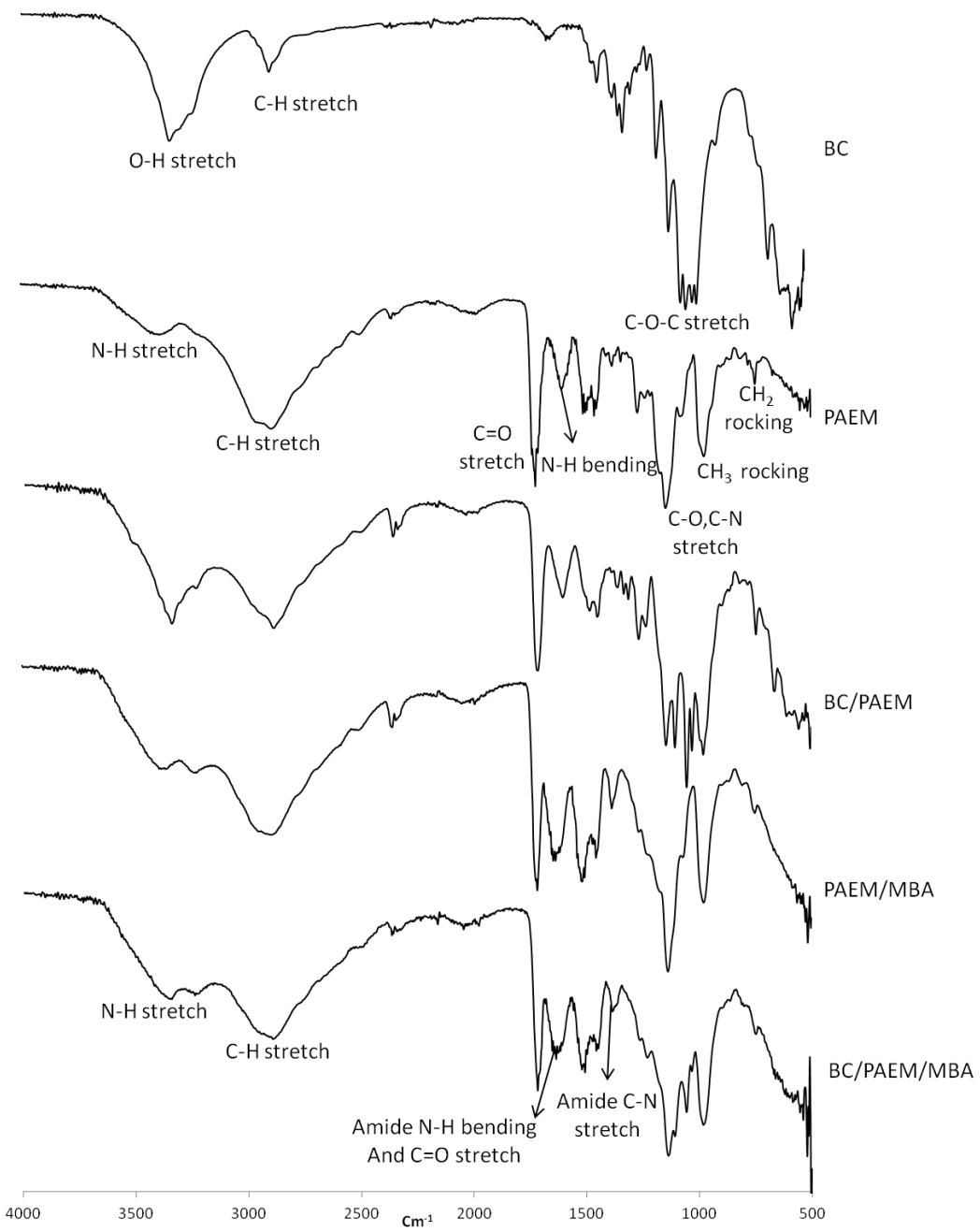

Figure 32 - ATR FT-IR spectra of bacterial cellulose (BC), BC/PAEM and BC/PAEM/MBA nanocomposites.

The FTIR spectra of BC/PAEM and BC/PAEM/MBA films correspond to the sum of the FTIR spectra of its components (BC and PAEM). The success of the PAEM polymerization inside the BC network was mainly confirmed by the appearance of an intense band at around 1717 cm^{-1}, associated to the C=O stretching vibrations of PAEM, and by the increase of the relative intensity of the region around 3500-2500 cm^{-1}, as a result of the increased number of aliphatic C-H vibrations resultant from polymer matrix and, in the particular case of BC/PAEM/MBA material, due to the crosslinker incorporation. This is further confirmed by the appearance of methacrylic polymers

characteristic bands around 1457 and 746 cm^{-1}, attributed to the CH_2 bending and CH_2 rocking vibrations.

Moreover, in BC/PAEM/MBA nanocomposite spectrum the profile around 1200-900 cm^{-1} is very similar to that of PAEM/MBA, as a result of the high polymer content in this material.

3.1.2. CP-MAS ^{13}C NMR

The CP-MAS ^{13}C NMR spectra of BC, PAEM, PAEM/MBA and BC/PAEM and BC/PAEM/MBA nanocomposites are shown in figure 33.

The NMR spectrum of PAEM is characterized by ^{13}C resonances at δ 19.1 (α-CH_3), 40.0 (quaternary carbon), 45.2 (CH_2 main chain), 54.4 (C-N) 62.5 (-O-CH_2) and 178.4 ppm (C=O) [75]. PAEM/MBA has a ^{13}C NMR spectrum very similar to that of PAEM. However, an increment of the resonance at δ 45.7 ppm is observed while the resonance at δ54.4 ppm is no longer observed, possibly due to overlapping with the resonance of the CH_2 groups. Furthermore, an increase of the resonance of the quaternary carbon (C*) and carbonyl groups (C=O) is also verified, resulting from the crosslinker incorporation.

The NMR spectrum of BC is characterized by ^{13}C resonances at δ 65.4 (C-6), 71.9-74.7 (C-2,3,5), 89.0 (C-4) and 105.2 ppm (C-1); which is in agreement with the values described in literature [32,75,92].

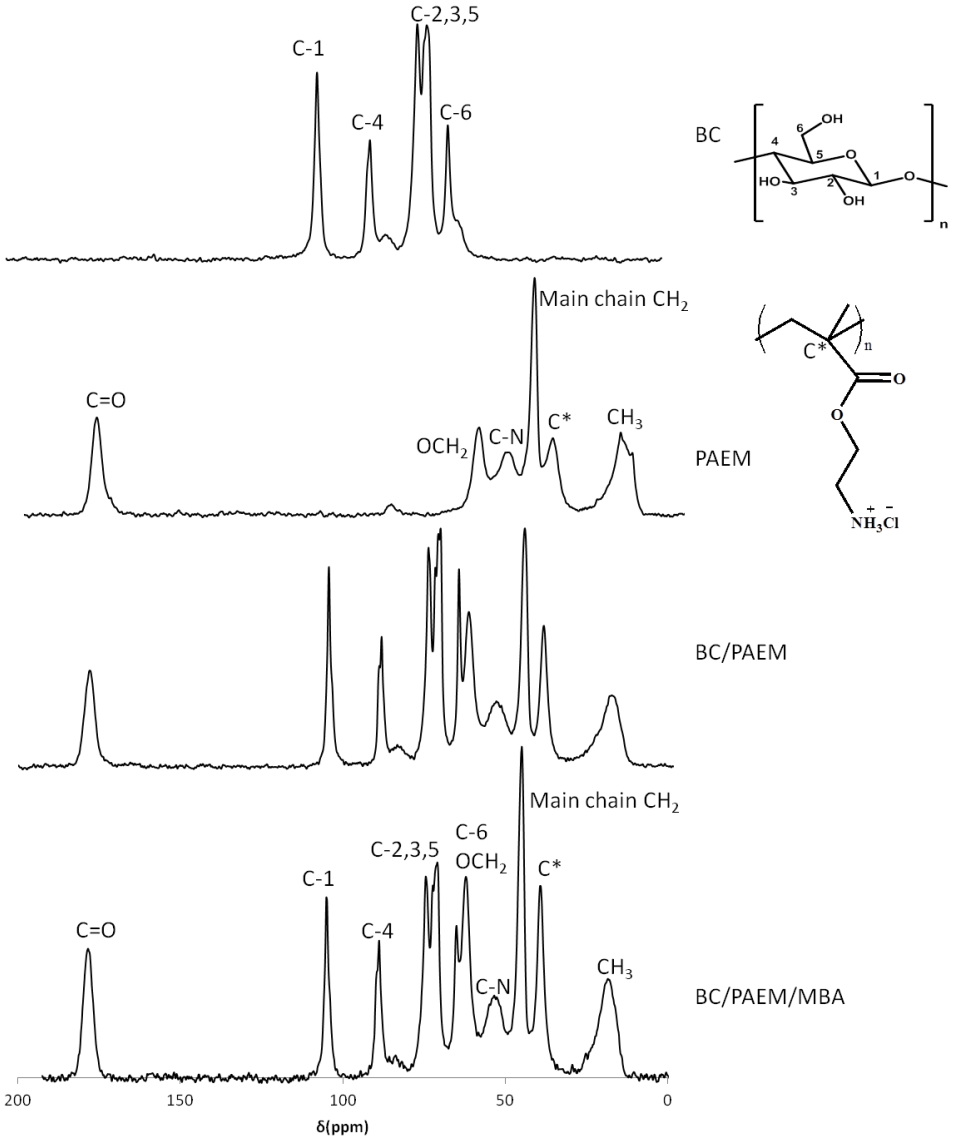

Figure 33 – CP-MAS ^{13}C NMR spectra of BC, BC/PAEM and BC/PAEM/MBA.

The ^{13}C NMR spectra of BC/PAEM and BC/PAEM/MBA nanocomposites are a result of the sum of the carbon resonances of BC and the corresponding acrylic polymer. In fact, all nanocomposites have a very similar profile. The only difference is the increased intensity of the resonances associated with quaternary carbons and CH_2 groups observed for the BC/PAEM/MBA nanocomposite, in comparison with the cellulose C-1 signal, resultant of the presence of crosslinker and the consequent increase of polymer content.

Furthermore, the absence of carbon resonances characteristic of the monomer (AEM) and particularly those associated with double bonds, demonstrates the complete polymerization of the monomer and/or effective removal of unreacted monomer or by-products during the washing procedure.

3.2. Morphological characterization

The morphology of bacterial cellulose membranes and each BC/PAEM nanocomposite material was analyzed through scanning electron microscopy (SEM), aiming to assess the dispersion of the polymer in the BC network. Selected SEM images of BC, BC/PAEM and BC/PAEM/MBA are shown in Figure 34.

Micrographs obtained for pure BC membranes reveals its well-known ultrafine network structure, composed of a random assembly of nanofibers, as well as its lamellar structure (cross-section images) [25,43,93].

SEM images of the nanocomposites further confirm the effectiveness of the polymerization reaction, with the polymer forming not only on the surface but also on the interior of the BC membrane. In fact, the cross-section micrographs of both nanocomposite films displayed the typical lamellar morphology of BC completely impregnated with PAEM, being the BC/PAEM/MBA dry film much thicker than the one obtained for BC/PAEM.

In the case of the surface micrographs the complete coating of the BC/PAEM/MBA material surface is observed, the opposite being verified for the BC/PAEM nanocomposite suggesting the lixiviation of the polymer during the washings. In fact, this difference may be the cause of the mass difference between the two nanocomposite materials.

The conclusions drawn from the SEM micrographs are in agreement with the results previously obtained through FT-IR, in which the BC/PAEM/MBA profile is very similar to that of PAEM/MBA while for the BC/PAEM there is a mixture of signals from both BC and PAEM; and ^{13}C NMR, according to which the BC/PAEM/MBA shows an increase of the carbon resonances derived from the polymer compared to the BC/PAEM spectrum.

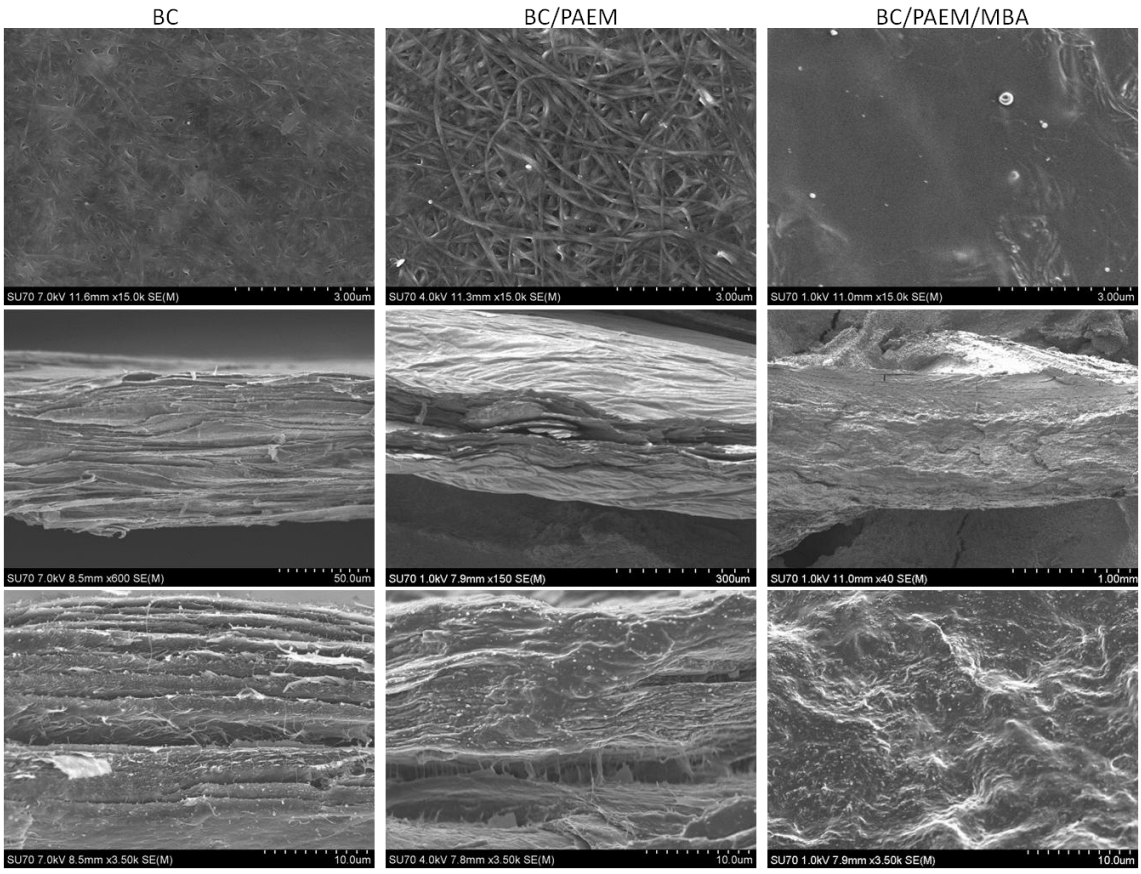

Figure 34 - Scanning electron microscopy images of BC (left), BC/PAEM (middle) and BC/PAEM/MBA (right). The surface images are presented on the first row while the cross-section images are shown below.

3.3. X-ray diffraction characterization

X-ray diffraction analyses have been performed on neat BC membranes, PAEM matrices (without and with 20% *w/w* crosslinker), BC/PAEM and BC/PAEM/MBA nanocomposite films (Figure 35) in order to assess the effect of the polymer incorporation in the crystallinity of BC membranes.

As well known, BC exhibits a diffractogram typical of Cellulose I (native cellulose), with the main peaks at 2θ 14.3, 16.8, 20.3, 22.6 and 34.0º [12,75,94], while PAEM and PAEM/MBA matrices display diffraction profiles typical of amorphous polymers.

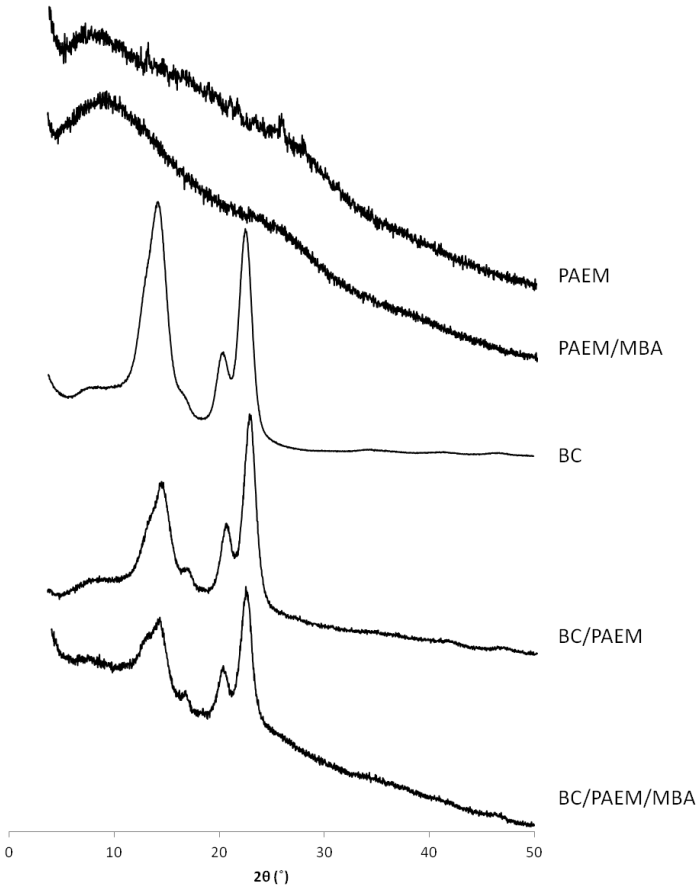

Figure 35 - X-Ray diffractograms of PAEM, PAEM/MBA, BC and the nanocomposites (BC/PAEM and BC/PAEM/MBA).

The X-ray diffraction profiles of the nanocomposite films show only the typical diffraction peaks of BC with decreased intensity, being this more evident for the peak at 2θ 14.3º. This decreased crystallinity is more evident for the BC/PAEM/MBA than for BC/PAEM nanocomposite, as a result of the higher

polymer content, and can be related to the decreased mechanical properties of the nanocomposites, as will be discussed below.

3.4.Swelling behavior

Swelling studies were performed for BC membrane (control sample) and BC/PAEM and BC/PAEM/MBA nanocomposite films in order to evaluate their re-hydration ability (reverse swelling after drying) after 48 h immersion in water (Figure 36).

All samples absorbed water during the experiment and have a similar pattern, showing high water uptake during the first hours followed by a decrease in the water absorption that lead to a plateau after 24 hours. However, the nanocomposite films have higher water uptake than the BC membrane, which is particularly evident for BC/PAEM.

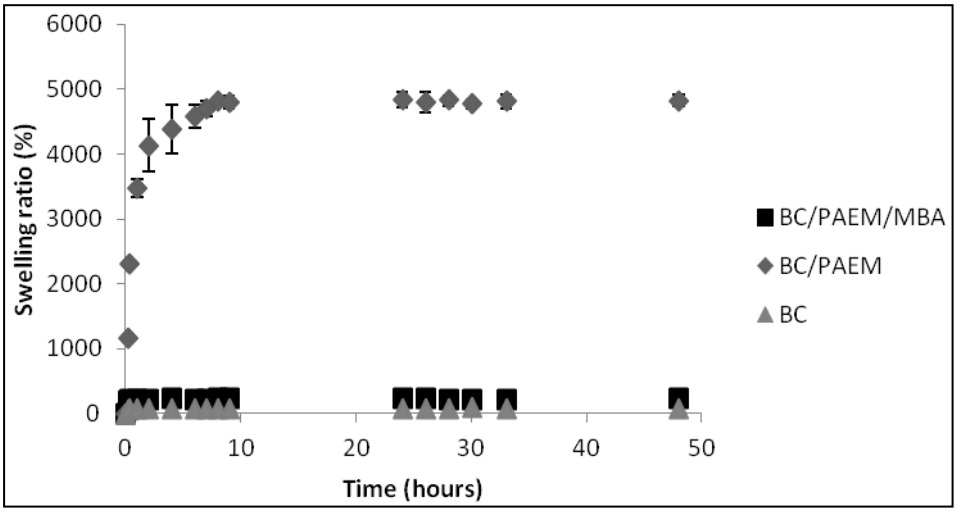

(a)

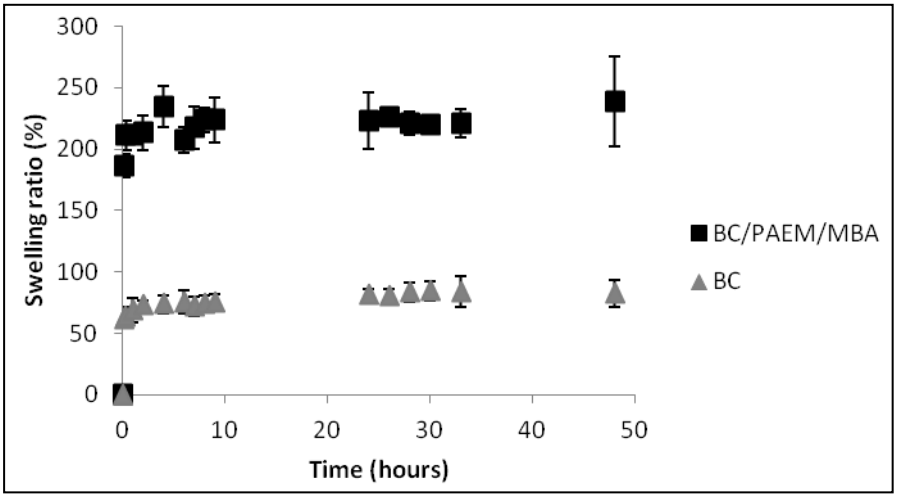

(b)

Figure 36 – (a) Graphic of the swelling ratio of BC/PAEM and BC/PAEM/MBA nanocomposite films and BC membrane (0-48 h). (b) Expansion of the BC and BC/PAEM/MBA swelling ratio graphic.

The BC/PAEM nanocomposite film has considerably higher water uptake than its cross-linked counterparts, with swelling ratios of 5300% and 230%, respectively, after 48 hours. Visual inspection of the samples (Figure 37) also shows appreciable increment of the nanocomposite films thickness, from around 0.05 cm (in the dry state) to 1.20 cm, in the case of BC/PAEM, and to 0.15 cm, in the case of BC/PAEM/MBA (when swollen).

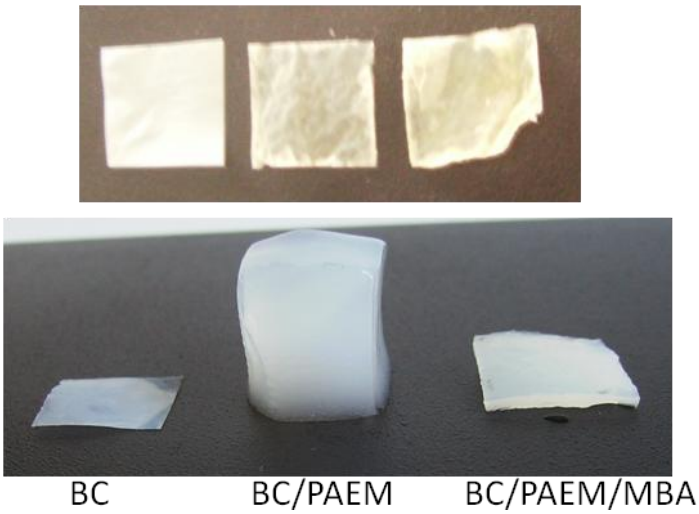

Figure 37 – Photographs of BC, BC/PAEM and BC/PAEM/MBA films in the dry (upper image) and swollen states (down image).

The behaviour of the BC/PAEM material is attributed to the hydrophilic character of BC, and particularly of PAEM. The presence of PAEM into the BC network prevents the collapse of the BC structure during drying and the existence of high number of hydrophilic ammonium groups in the structure favours the water uptake.

In the case of BC/PAEM/MBA, the high content of crosslinker incorporated formed a more rigid and condensed polymeric network which restricts the inter-chain movement and possibly hinders the swelling of the material [95–97].

The high water swelling, mainly of BC/PAEM, is particularly important in biomedical applications of the material, namely as wound dressing, in order to provide a wet environment that favours tissue healing as well as in the wound exudates absorption.

3.5.Thermogravimetric analysis (TGA)

The TGA of BC/PAEM nanocomposites was used to investigate their thermal stability and degradation profiles. Reference BC membrane and PAEM matrices (with and without crosslinker) were also analysed for comparison purposes (Table 3, Figure 38).

The pristine BC membrane displayed a typical single mass-loss step degradation profile, initiating its thermal decomposition at 260ºC and reaching maximum decomposition rate at 350 ºC [98] with 94% mass loss. The mass loss at around 66ºC is associated with the volatilization of residual water.

Both PAEM and PAEM/MBA are less thermally stable than BC (Figure 38). However, PAEM/MBA is slightly more stable than PAEM, since its first maximum degradation occurs at a temperature 30ºC higher than that of PAEM. So, as expected, the crosslinking process increases the thermal stability of the polymer. This is further confirmed by the fact that in the first degradation step PAEM lost 49.5% of its weight while for PAEM/MBA the loss was of 39.4%.

As it can be seen (Figure 38), the TGA tracings of PAEM and PAEM/MBA reveal a three-step weight loss, occurring at around 300, 430 and 580ºC. Following the data described for similar poly(methacrylates) containing amine side groups [99,100], the first degradation step can be ascribed to the main chain depolymerization, yielding monomers and oligomers. During the second degradation step there is the cleavage of the ester linkage and, finally, the third step is associated to the carbonization process of the remaining products.

In the case of the BC nanocomposites, their TGA profile is not the sum of the profiles of the individual components. Both nanocomposites show a multi-step degradation profile, very similar to that of the corresponding pristine polymer. However, in both nanocomposites, the polymer incorporation into the BC network resulted in improved thermal stability, in comparison with the pristine polymers (Table 3), as a result of the establishment of interactions between the components.

Furthermore, the thermal stability of BC/PAEM and BC/PAEM/MBA nanocomposites around 120ºC, the temperature involved in typical sterilization procedures required for biomedical applications, allows these materials to undergo this process.

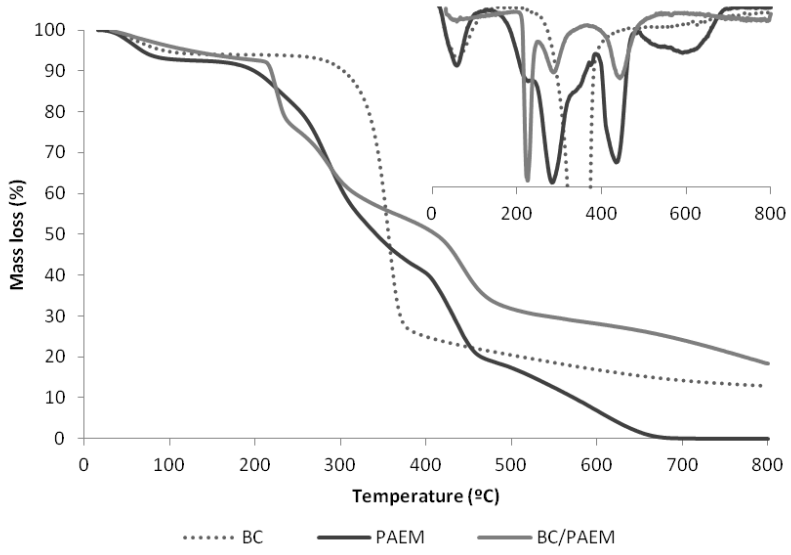

(a)

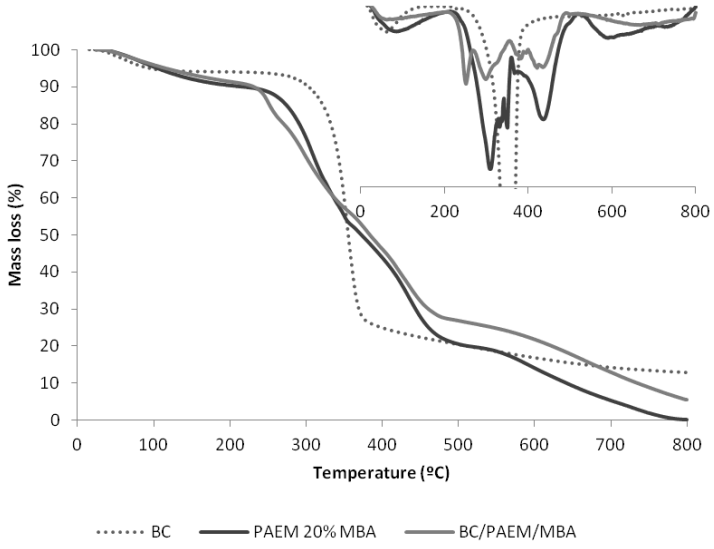

(b)

Figure 38 – TGA thermographs of (a) BC, PAEM and BC/PAEM and (b) BC, PAEM/MBA and BC/PAEM/MBA.

Table 3 – Thermal properties of pristine bacterial cellulose (BC), polymer (PAEM), cross-linked polymer (PAEM/MBA) and the BC-based nanocomposites.

Material	Tdi[a] (ºC)	Tdmax1[b] (ºC)	Tdmax2[b] (ºC)	Tdmax3[b] (ºC)	Tdmax4[b] (ºC)
BC	260	353	-	-	-
PAEM	128	279	429	587	-
BC/PAEM	195	223	279	435	-
PAEM/MBA	210	307	431	585	-
BC/PAEM/MBA	200	248	292	378	419, 425

[a] Temperature at the beginning of the degradation

[b] Maximum degradation temperature

3.6. Mechanical analysis

Tensile tests were performed, at room temperature, for BC and all nanocomposites. Figure 39 shows the tensile mechanical properties, including Young's modulus (E), tensile strength and elongation at break, determined from the typical stress-strain curves.

Tensile test of the pristine polymers was not possible due to their brittleness. However, polymer incorporation into the BC membrane produced nanocomposite materials with measurable mechanical properties, therefore with increased mechanical properties this way confirming BC efficiency as a reinforcement of polymers [42,65,67].

Besides, comparing BC/PAEM and BC/PAEM/MBA, it is found that BC/PAEM has better mechanical properties than those of BC/PAEM/MBA, possibly as a result of the lower polymer content. Such difference is also a result of crosslinker incorporation into BC/PAEM/MA material, which produces a stiffer polymer more easily deformed when subjected to tensile strength.

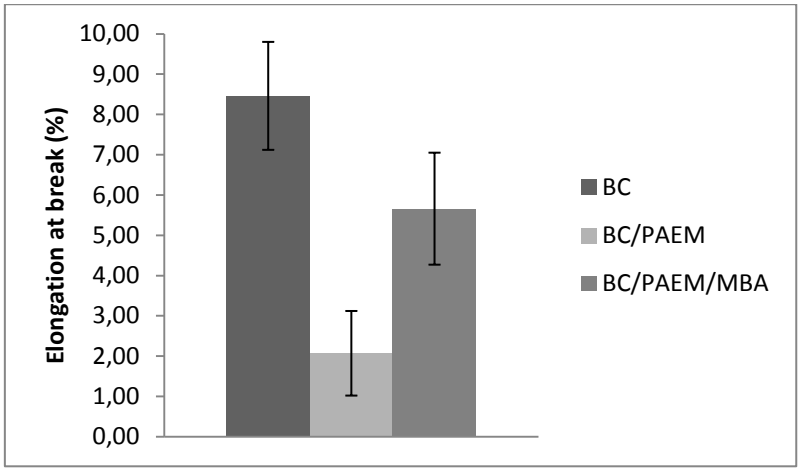

(a)

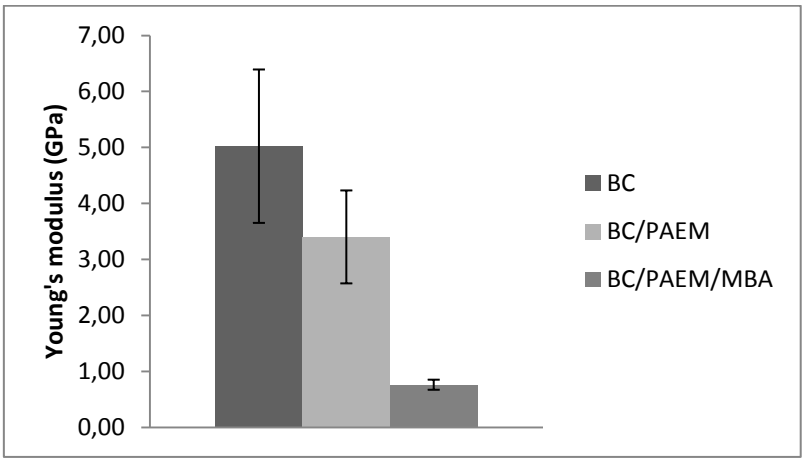

(b)

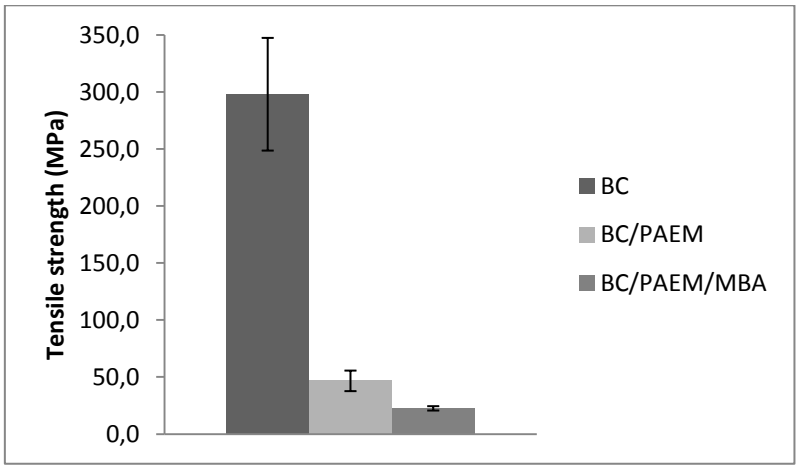

(c)

Figure 39 – Elongation at break (a), Young's modulus (b) and tensile strength (c) of pristine bacterial cellulose (BC) and the BC-based nanocomposites: BC/PAEM and BC/PAEM/MBA.

3.7. Antimicrobial properties assessment

The existence of ammonium groups in the chemical structure of the PAEM polymer makes it, as well as the corresponding nanocomposite materials, potential biocidal agents. Therefore this hypothesis was evaluated by placing BC, PAEM (with and without crosslinker) and BC/PAEM and BC/PAEM/MBA nanocomposites in contact with a bacterial suspension of the bioluminescent *Escherichia coli* in tryptic soy broth (TSB). The visual aspect of an overnight *E. coli* liquid culture is shown in Figure 40.

Figure 40 – Visual aspect of an overnight liquid culture of bioluminescent *E. coli* [101].

The bacterial bioluminescent method is considered a rapid, sensitive and cost-effective option to the laborious conventional methods of plating, overnight incubation and time-consuming counting of colony-forming units (CFU). Moreover, it allows only living or viable cells to be detected and does not need exogenous administration of substrates to obtain light emission [88].

This method has been previously employed, among many others, in the evaluation of the antibacterial actions of whole herb tinctures [102] and to evaluate the photoinactivation ability of porphyrins [88]. These particular studies had the maximum duration of 4.5 hours, while our study was intended to last for 24 hours. Therefore, some optimization was required prior to the study.

Initially, following the procedure employed by Alves et al. [88], a bacterial suspension in phosphate buffered saline (PBS) was prepared and the bioluminescent signal was periodically measured during 24 hours (Figure 41). The results show the bioluminescent signal decreasing over time, probably as a result of the inexistence of

carbon sources that allowed the normal functioning of bacteria, and therefore this approach could not be employed.

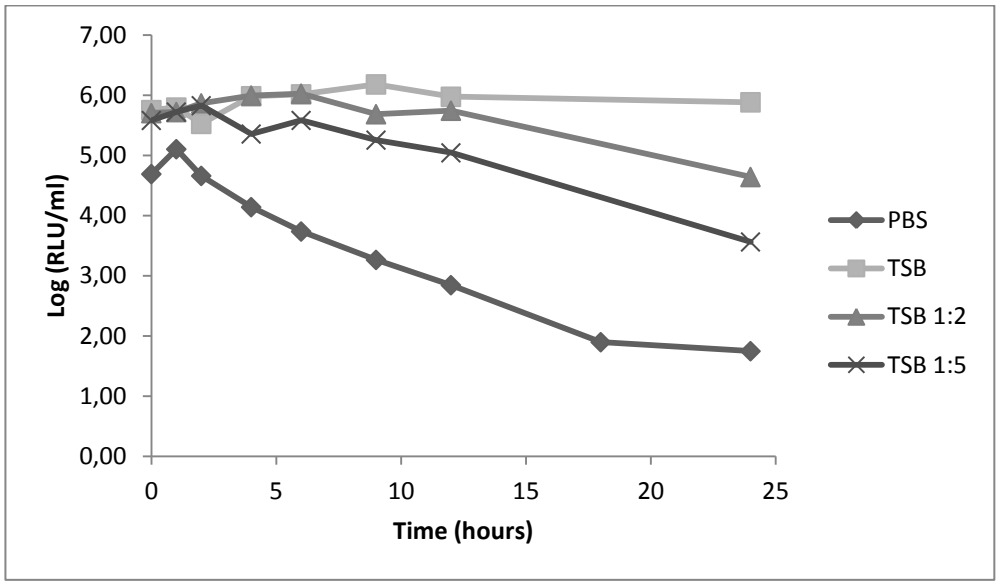

Figure 41 – Bioluminescent signal of *E. coli* liquid suspensions preliminary tests to evaluate the bacteria stability during 24 hours. Bacterial suspensions were prepared by tenfold diluting an overnight grown bacterial culture in phosphate buffered saline (PBS), tryptic soy broth (TSB) and TSB diluted twofold and fivefold.

Therefore the strategy was changed and the bacterial suspension was prepared in TSB culture medium diluted 1:2 and 1:5 and undiluted. The bioluminescent signal of the bacterial suspensions using diluted TSB showed a similar profile to that observed when using PBS, but with a smaller bioluminescence decrease. In the case of using undiluted TSB the bioluminescence signal remained constant over 24 hours and therefore that was considered the best approach for the determination of the antibacterial activity of the materials under test.

Finally, prior to the materials testing the correlation between the bioluminescent signal (RLU) and the viable counts (CFU) of overnight cultures of bioluminescent *E. coli* was evaluated. A linear relationship between the two variables was observed, revealing that 10^7 CFU mL^{-1} correspond, approximately, to 10^4 RLU mL^{-1} (Figure 42).

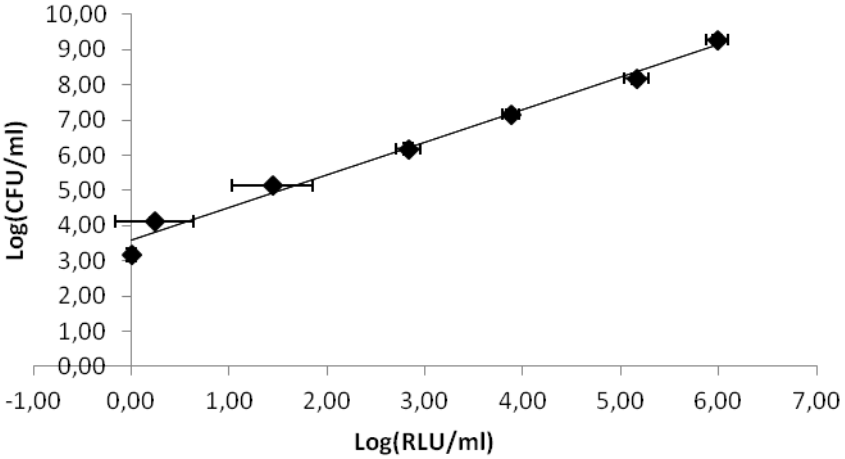

Figure 42 - Relationship between the bioluminescence signal and viable counts of overnight cultures of recombinant bioluminescent *E. coli* serially diluted in PBS. Viable counts are expressed in CFU mL^{-1} and bioluminescence in relative light units (RLU). Each value represents mean ± standard deviation of three independent experiments.

The results of the antibacterial activity tests of BC, PAEM, PAEM/MBA and the corresponding nanocomposites are shown in figure 43. As expected [63], bacterial cellulose (BC) has no effect on the bacterial viability, with the bioluminescence values being similar to those of the control sample.

The antibacterial activity of the materials being tested is expected to be a result of the interaction between the ammonium groups of the polymer with bacteria. In the case of PAEM this appears to happen once it causes total bacteria death in the first contact hours.

The incorporation of PAEM inside the BC network, creating the BC/PAEM nanocomposite, does not affect its ability to kill bacteria. In fact this activity is extended for more 18 hours, which may be useful when the aim is to develop a material with prolonged activity. The high swelling ability of this material contributes to the diffusion of bacterial suspension into the nanocomposite material therefore promoting the contact between the pendant ammonium groups and bacteria and finally causing bacterial death.

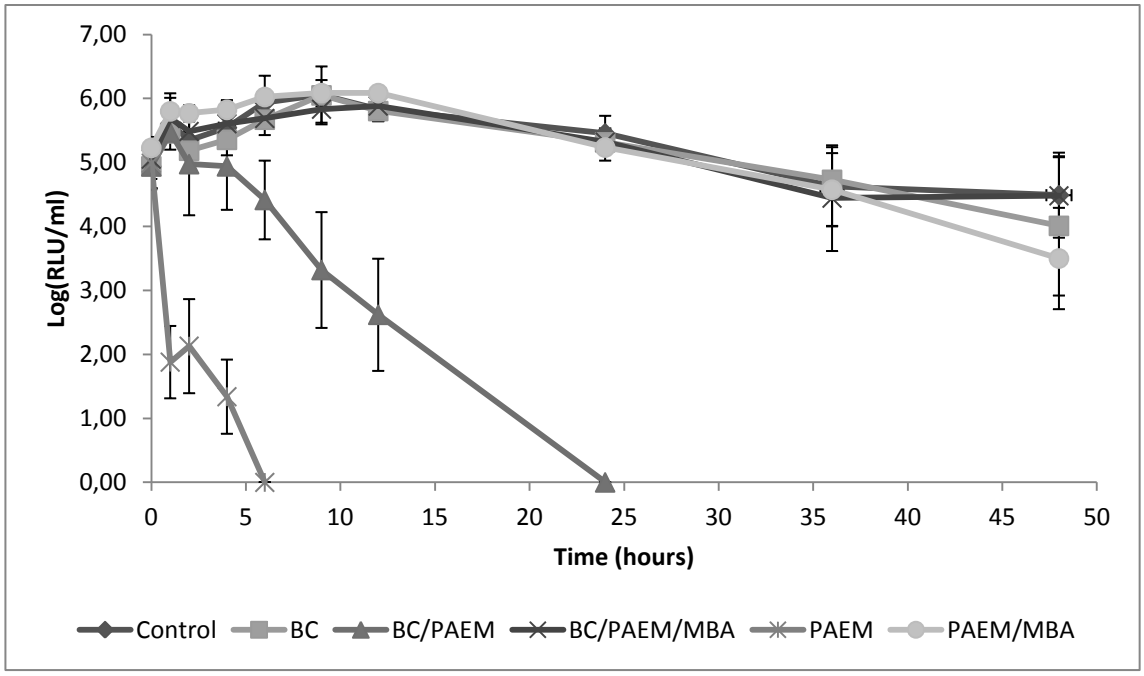

Figure 43 – Bioluminescent signal of *E. coli* liquid suspensions in TSB after 0,1,2,4,6,9,12,24,36 and 48 hours of contact with PAEM, PAEM/MBA, BC, BC/PAEM or BC/PAEM/MBA. A control sample is also shown, for comparison, consisting of a tenfold diluted *E.coli* liquid suspension in TSB.

PAEM/MBA, on the other hand, shows a slight activity only after 48 hours of contact with bacteria. Such reduced antibacterial activity seems to be a result of the crosslinking reaction, from which a much rigid polymer is generated that hinders its swelling ability. This process may also alter ammonium groups organization in such a way that there may be hindrance in the contact of the ammonium groups with bacterial cells.

The BC/PAEM/MBA nanocomposite, as its corresponding polymer, has no detectable antibacterial activity showing a behavior similar to that of control and BC samples. This lack of activity can be justified by the same reasons stated above for PAEM/MBA. Furthermore, the enclosure of PAEM/MBA into the BC network together with its hindrance towards the nanocomposite swelling makes the contact of ammonium groups and bacteria even smaller.

4. Conclusions

The present work describes the successful preparation of bacterial cellulose and poly(2-aminoethyl methacrylate) (BC/PAEM) nanocomposite materials, with and without crosslinker, through *in situ* polymerization.

The polymer incorporation into the BC membranes produced the total filling of BC porous structure and increased its mechanical properties as a result of BC reinforcing ability. Furthermore, the crystallinity of the ensuing materials is decreased, in comparison with that of pure BC, due to the high amorphous polymer content in the material.

In addition, the polymer incorporation into the BC membrane increased its swelling ability once it prevents the collapse of the BC structure, being this more evident for BC/PAEM. The BC/PAEM is also the nanocomposite with higher antibacterial activity towards bioluminescent *E. coli*, in contrast with its cross-linked counterparts with no detectable antibacterial activity.

Following what was described before, this novel material allowed imparting antimicrobial activity to BC membranes.

From the nanocomposite materials developed, BC/PAEM is the one with better properties. This way it has potential to be tested in wound dressing, simultaneously creating a moist environment, that favors wound healing, and inhibiting the development of bacterial infections. Its high swelling ability might also help the absorption of wound exudates, this way further favoring wound healing.

Finally, future research activities to continue this study will involve some of the following aspects:

-The tuning of the crosslinking agent content (and eventually its nature) in order to tune the swelling behavior of the membrane, while preserving its biological activity;

-The evaluation of the biocompatibility of the nanocomposites materials in order to validate their potential to be used in biomedical devices;

-Testing the potential of these new membranes as drug delivery systems (eg. for anti-inflammatory or pain relief drugs or eventually antibiotics). .

5. Bibliography

1. Belgacem, M. N.; Gandini, A. in *Monomers, Polymers and composites from Renewable Resources* (Belgacem, M. N.; Gandini, A.) (Elsevier Ltd., 2008).

2. Gandini, A. Polymers from Renewable Resources: A Challenge for the Future of Macromolecular Materials. *Macromolecules* **41,** 9491–9504 (2008).

3. Doerell, P. E. All future energy will have to be clean. **64,** 79–88 (1999).

4. Dufresne, A. in *Monomers, Polymers and Composites from Renewable Resources* (Belgacem, M. N.; Gandini, A.) (Elsevier Ltd., 2008).

5. Huber, T. *et al.* A critical review of all-cellulose composites. *Journal of Materials Science* **47,** 1171–1186 (2011).

6. Freire, C., Fernandes, S., Silvestre, A. & Neto, P. Novel cellulose-based composites based on nanofibrillated plant and bacterial cellulose: recent advances at the University of Aveiro – a review. *Holzforschung - International Journal of the Biology, Chemistry, Physics, and Technology of Wood* **0,** 1–10 (2012).

7. Kalia, S. *et al.* Cellulose-Based Bio- and Nanocomposites: A Review. *International Journal of Polymer Science* 1–35 (2011).

8. Klemm, D., Schumann, D., Udhardt, U. & Marsch, S. Bacterial synthesized cellulose — artificial blood vessels for microsurgery. *Progress in Polymer Science* **26,** 1561–1603 (2001).

9. Jonas, R. & Farah, L. F. Production and application of microbial cellulose. *Polymer Degradation and Stability* **59,** 101–106 (1998).

10. Vandamme, E. J., De Baets, S., Vanbaelen, A., Joris, K. & De Wulf, P. Improved production of bacterial cellulose and its application potential. *Polymer Degradation and Stability* **59,** 93–99 (1998).

11. Pérez, S. & Mazeau, K. in *Polysaccharides, Structural Diversity and Functional Versatility* (Dimitriu, S.) 41–68 (Marcel Dekker, 2005).

12. Klemm, D., Heublein, B., Fink, H.-P. & Bohn, A. Cellulose: fascinating biopolymer and sustainable raw material. *Angewandte Chemie (International ed. in English)* **44,** 3358–93 (2005).

13. Sadava, D., Heller, H. C., Hillis, D. M. & Berenbaum, M. *Life:The Science of Biology*. (2009).

14. Voragen, A. G. J., Coenen, G.-J., Verhoef, R. P. & Schols, H. a. Pectin, a versatile polysaccharide present in plant cell walls. *Structural Chemistry* **20,** 263–275 (2009).

15. Klemm, D. *et al.* Nanocelluloses as Innovative Polymers in Research and Application. *Advances in Polymer Science* **205,** 49–96 (2006).

16. Chawla, P. R., Bajaj, I. B., Survase, S. A. & Singhal, R. S. Microbial Cellulose : Fermentative Production and Applications. *Food Technology and Biotecnology* **47,** 107–124 (2009).

17. Sullivan, A. C. O. Cellulose : the structure slowly unravels. *Cellulose* **4,** 173–207 (1997).

18. Lavoine, N., Desloges, I., Dufresne, A. & Bras, J. Microfibrillated cellulose - its barrier properties and applications in cellulosic materials: a review. *Carbohydrate polymers* **90,** 735–64 (2012).

19. Azizi Samir, M. A. S., Alloin, F. & Dufresne, A. Review of recent research into cellulosic whiskers, their properties and their application in nanocomposite field. *Biomacromolecules* **6,** 612–26 (2005).

20. Zimmermann, T., Bordeanu, N. & Strub, E. Properties of nanofibrillated cellulose from different raw materials and its reinforcement potential. *Carbohydrate Polymers* **79,** 1086–1093 (2010).

21. Verlhac, C., Dedier, J. & Chanzy, H. Availability of surface hydroxyl groups in valonia and bacterial cellulose. *Journal of Polymer Science Part A: Polymer Chemistry* **28,** 1171–1177 (1990).

22. Eichhorn, S. J. *et al.* Review: current international research into cellulose nanofibres and nanocomposites. *Journal of Materials Science* **45,** 1–33 (2010).

23. Office of Biological and Environmental Research of the U.S. Department of Energy Office of Science. *Cellulose Structure and Hydrolysis Challenges* at <https://public.ornl.gov/site/gallery/detail.cfm?id=181&topic=&citation=&general=plant cell wall&restsection=all>

24. Nishiyama, Y., Sugiyama, J., Chanzy, H. & Langan, P. Crystal structure and hydrogen bonding system in cellulose Iα from synchrotron x-ray and neutron fiber diffraction. *Journal of the American Chemical Society* **125,** 14300–14306 (2003).

25. Klemm, D. *et al.* Nanocelluloses: a new family of nature-based materials. *Angewandte Chemie (International ed. in English)* **50,** 5438–66 (2011).

26. Trovatti, E., Serafim, L. S., Freire, C. S. R., Silvestre, A. J. D. & Neto, C. P. Gluconacetobacter sacchari: An efficient bacterial cellulose cell-factory. *Carbohydrate Polymers* **86,** 1417–1420 (2011).

27. Nge, T. T., Sugiyama, J. & Bulone, V. in *Biopolymers* (Elnashar, M.) 345–368 (InTech, 2010).

28. Helenius, G. *et al.* In vivo biocompatibility of bacterial cellulose. *Journal of Biomedical Materials Research Part A* **76,** 431–438 (2006).

29. Iguchi, M., Yamanaka, S. & Budhiono, A. Bacterial cellulose — a masterpiece of nature ' s arts. *Journal of Materials Science.* **35,** 261–270 (2000).

30. Torres, F. G., Troncoso, O. P., Lopez, D., Grande, C. & Gomez, C. M. Reversible stress softening and stress recovery of cellulose networks. *Soft Matter* **5,** 4185–4190 (2009).

31. Cheng, K.-C., Catchmark, J. M. & Demirci, A. Effect of different additives on bacterial cellulose production by Acetobacter xylinum and analysis of material property. *Cellulose* **16,** 1033–1045 (2009).

32. Watanabe, K., Tabuchi, M., Morinaga, Y. & Yoshinaga, F. Structural features and properties of bacterial cellulose produced in agitated culture. *Cellulose* **5,** 187–200 (1998).

33. Czaja, W., Romanovicz, D. & Brown, R. M. Structural investigations of microbial cellulose produced in stationary and agitated culture. *Cellulose* **11,** 403–411 (2004).

34. Hu, Y. & Catchmark, J. M. Formation and characterization of spherelike bacterial cellulose particles produced by Acetobacter xylinum JCM 9730 strain. *Biomacromolecules* **11,** 1727–1734 (2010).

35. El-Saied, H., Basta, A. H. & Gobran, R. H. Research Progress in Friendly Environmental Technology for the Production of Cellulose Products (Bacterial Cellulose and Its Application). *Polymer-Plastics Technology and Engineering* **43,** 797–820 (2004).

36. Czaja, W., Krystynowicz, A., Bielecki, S. & Brown, R. M. Microbial cellulose--the natural power to heal wounds. *Biomaterials* **27,** 145–51 (2006).

37. Siró, I. & Plackett, D. Microfibrillated cellulose and new nanocomposite materials: a review. *Cellulose* **17,** 459–494 (2010).

38. Carreira, P. *et al.* Utilization of residues from agro-forest industries in the production of high value bacterial cellulose. *Bioresource Technology* **102,** 7354–60 (2011).

39. Vazquez, A., Foresti, M. L., Cerrutti, P. & Galvagno, M. Bacterial Cellulose from Simple and Low Cost Production Media by Gluconacetobacter xylinus. *Journal of Polymers and the Environment* **21,** 545–554 (2012).

40. Castro, C. *et al.* Structural characterization of bacterial cellulose produced by Gluconacetobacter swingsii sp. from Colombian agroindustrial wastes. *Carbohydrate Polymers* **84,** 96–102 (2011).

41. Yamanaka, S. *et al.* The structure and mechanical properties of sheets prepared from bacterial cellulose. *Journal of Materials Science* **24,** 3141–3145 (1989).

42. Kim, Y., Jung, R., Kim, H.-S. & Jin, H.-J. Transparent nanocomposites prepared by incorporating microbial nanofibrils into poly(l-lactic acid). *Current Applied Physics* **9,** S69–S71 (2009).

43. Hofinger, M., Bertholdt, G. & Weuster-Botz, D. Microbial production of homogeneously layered cellulose pellicles in a membrane bioreactor. *Biotechnology and Bioengineering* **108,** 2237–2240 (2011).

44. Kim, J. *et al.* Preparation and characterization of a Bacterial cellulose/Chitosan composite for potential biomedical application. *Journal of Polymer Research* **18,** 739–744 (2010).

45. Cai, Z. & Kim, J. Bacterial cellulose/poly(ethylene glycol) composite: characterization and first evaluation of biocompatibility. *Cellulose* **17,** 83–91 (2010).

46. Shi, Z. *et al.* In situ nano-assembly of bacterial cellulose–polyaniline composites. *RSC Advances* **2,** 1040–1046 (2012).

47. Lina, F., Yue, Z., Jin, Z. & Guang, Y. in *Biomedical Engineering - Frontiers and Challenges* (Fazel, P. R.) 249–274 (InTech, 2011).

48. White, D. G. & R. M. Brown, J. in *Cellulose and Wood -Chemistry and Technology* (Schuerch, C.) (John Wiley and Sons, Inc., 1989).

49. Akbar, A. BISMA center.

50. Amnuaikit, T., Chusuit, T., Raknam, P. & Boonme, P. Effects of a cellulose mask synthesized by a bacterium on facial skin characteristics and user satisfaction. *Medical Devices: Evidence and Research* **4,** 77–81 (2011).

51. Hasan, N. & Biak, Dayang Radiah Awang Kamarudin, S. Application of Bacterial Cellulose (BC) in Natural Facial Scrub. *International Journal on Advanced Science, Engineering Information Technology* **2,** (2012).

52. Heath, Benjamin Parker Coffindaffer, T. W. & Kyte, Kenneth Eugene Smith, Edward Dewey McConaughy, S. D. Personal cleansing compositions comprising bacterial cellulose network and cationic polymer. (2010).

53. Pecoraro, É., Manzani, D., Messaddeq, Y. & J.L.Ribeiro, S. in *Monomers, Polymers and Composited from Renewable Resources* (Gandini, A.) 369–374 (Elsevier, 2008).

54. Trovatti, E. *et al.* Bacterial cellulose membranes applied in topical and transdermal delivery of lidocaine hydrochloride and ibuprofen: In vitro diffusion studies. *International Journal of Pharmaceutics* **435,** 83–87 (2012).

55. Trovatti, E. *et al.* Biocellulose membranes as supports for dermal release of lidocaine. *Biomacromolecules* **12,** 4162–8 (2011).

56. Azeredo, H. M. C. De. Nanocomposites for food packaging applications. *Food Research International* **42,** 1240–1253 (2009).

57. Zhu, H. *et al.* Biosynthesis of spherical Fe3O4/bacterial cellulose nanocomposites as adsorbents for heavy metal ions. *Carbohydrate Polymers* **86,** 1558–1564 (2011).

58. Yano, S., Maeda, H., Nakajima, M., Hagiwara, T. & Sawaguchi, T. Preparation and mechanical properties of bacterial cellulose nanocomposites loaded with silica nanoparticles. *Cellulose* **15,** 111–120 (2008).

59. Gea, S., Bilotti, E., Reynolds, C. T., Soykeabkeaw, N. & Peijs, T. Bacterial cellulose–poly(vinyl alcohol) nanocomposites prepared by an in-situ process. *Materials Letters* **64,** 901–904 (2010).

60. Zhijiang, C., Guang, Y. & Kim, J. Biocompatible nanocomposites prepared by impregnating bacterial cellulose nanofibrils into poly(3-hydroxybutyrate). *Current Applied Physics* **11,** 247–249 (2011).

61. Barud, H. S. *et al.* Bacterial cellulose/poly(3-hydroxybutyrate) composite membranes. *Carbohydrate Polymers* **83,** 1279–1284 (2011).

62. Maneerung, T., Tokura, S. & Rujiravanit, R. Impregnation of silver nanoparticles into bacterial cellulose for antimicrobial wound dressing. *Carbohydrate Polymers* **72,** 43–51 (2008).

63. Pinto, R. J. B. *et al.* Antibacterial activity of nanocomposites of silver and bacterial or vegetable cellulosic fibers. *Acta Biomaterialia* **5,** 2279–2289 (2009).

64. Hu, W. *et al.* In situ synthesis of silver chloride nanoparticles into bacterial cellulose membranes. *Materials Science and Engineering: C* **29,** 1216–1219 (2009).

65. Martins, I. M. G. *et al.* New biocomposites based on thermoplastic starch and bacterial cellulose. *Composites Science and Technology* **69,** 2163–2168 (2009).

66. Tome, L. C. *et al.* Transparent bionanocomposites with improved properties prepared from acetylated bacterial cellulose and poly(lactic acid) through a simple approach. *Green Chemistry* **13,** 419–427 (2011).

67. Fernandes, S. C. M. *et al.* Novel transparent nanocomposite films based on chitosan and bacterial cellulose. *Green Chemistry* **11,** 2023–2029 (2009).

68. Trovatti, E. *et al.* Novel bacterial cellulose–acrylic resin nanocomposites. *Composites Science and Technology* **70,** 1148–1153 (2010).

69. Trovatti, E. *et al.* Sustainable nanocomposite films based on bacterial cellulose and pullulan. *Cellulose* **19,** 729–737 (2012).

70. Marins, J. A. *et al.* Structure and properties of conducting bacterial cellulose-polyaniline nanocomposites. *Cellulose* **18,** 1285–1294 (2011).

71. Muller, D. *et al.* Electrically conducting nanocomposites: preparation and properties of polyaniline (PAni)-coated bacterial cellulose nanofibers (BC). *Cellulose* **19,** 1645–1654 (2012).

72. Hobzova, R., Duskova-Smrckova, M., Michalek, J., Karpushkin, E. & Gatenholm, P. Methacrylate hydrogels reinforced with bacterial cellulose. *Polymer International* **61,** 1193–1201 (2012).

73. Kramer, F. *et al.* Nanocellulose Polymer Composites as Innovative Pool for (Bio)Material Development. *Macromolecular Symposia* **244,** 136–148 (2006).

74. Figueiredo, A. G. P. R. *et al.* Biocompatible Bacterial Cellulose–Poly(2-hydroxyethyl methacrylate) Nanocomposite Films. *BioMed Research International* (2013).

75. Lacerda, P. S. S., Barros-Timmons, A. M. M. V., Freire, C. S. R., Silvestre, A. J. D. & Neto, C. P. Nanostructured Composites Obtained by ATRP Sleeving of Bacterial Cellulose Nanofibers with Acrylate Polymers. *Biomacromolecules* **14,** 2063–2073 (2013).

76. Thompson, K. L., Read, E. S. & Armes, S. P. Chemical degradation of poly(2-aminoethyl methacrylate). *Polymer Degradation and Stability* **93,** 1460–1466 (2008).

77. Read, E. S., Thompson, K. L. & Armes, S. P. Synthesis of well-defined primary amine-based homopolymers and block copolymers and their Michael addition reactions with acrylates and acrylamides. *Polymer Chemistry* **1,** 221–230 (2010).

78. He, L., Read, E. S., Armes, S. P. & Adams, D. J. Direct Synthesis of Controlled-Structure Primary Amine-Based Methacrylic Polymers by Living Radical Polymerization. *Macromolecules* **40,** 4429–4438 (2007).

79. Ji, W., Panus, D., Palumbo, R. N., Tang, R. & Wang, C. Poly(2-aminoethyl methacrylate) with Well-Defined Chain Length for DNA Vaccine Delivery to Dendritic Cells. *Biomacromolecules* **12,** 4373–4385 (2011).

80. Jianxun, D. *et al.* Facile preparation of a cationic poly(amino acid) vesicle for potential drug and gene co-delivery. *Nanotechnology* **22,** 4940–4912 (2011).

81. Deng, K. L., Tian, H., Zhang, P. F., Ren, X. B. & Zhong, H. B. Synthesis and characterization of a novel temperature-pH responsive copolymer of 2-hydroxypropyl acrylate and aminoethyl methacrylate hydrochloric salt. *Express Polymer Letters* **3,** 97–104 (2009).

82. Kadokawa, J., Saitou, S. & Shoda, S. Preparation of polysaccharide–polymethacrylate hybrid materials by radical polymerization of cationic methacrylate monomer in the presence of anionic polysaccharide. *Polymers for Advanced Technologies* **18,** 643–646 (2007).

83. Kadokawa, J., Saitou, S. & Shoda, S. Preparation of alginate-polymethacrylate hybrid material by radical polymerization of cationic methacrylate monomer in the presence of sodium alginate. *Carbohydrate Polymers* **60,** 253–258 (2005).

84. Ionov, L., Synytska, A., Kaul, E. & Diez, S. Protein-Resistant Polymer Coatings Based on Surface-Adsorbed Poly(aminoethyl methacrylate)/Poly(ethylene glycol) Copolymers. *Biomacromolecules* **11,** 233–237 (2009).

85. Ekblad, T., Andersson, O., Tai, F.-I., Ederth, T. & Liedberg, B. Lateral Control of Protein Adsorption on Charged Polymer Gradients. *Langmuir* **25,** 3755–3762 (2009).

86. Geurts, J. M. *et al.* Syntheses of new amino-functionalized methacrylates and their use in free radical polymerizations. *Journal of Applied Polymer Science* **80,** 1401–1415 (2001).

87. Yuting, L. & Steven, P. A. Synthesis of Model Primary Amine-Based Branched Copolymers by Pseudo-Living Radical Copolymerization and Post-polymerization Coupling of Homopolymers. *Macromolecules* **42,** 939–945 (2009).

88. Alves, E. *et al.* Photodynamic inactivation of recombinant bioluminescent Escherichia coli by cationic porphyrins under artificial and solar irradiation. *Journal of Industrial Microbiology & Biotechnology* **35,** 1447–1454 (2008).

89. Halib, N., Amin, M. C. I. M. & Ahmad, I. Physicochemical Properties and Characterization of Nata de Coco from Local Food Industries as a Source of Cellulose. *Sains Malaysiana* **41,** 205–211 (2012).

90. Goh, W. N. *et al.* Microstructure and physical properties of microbial cellulose produced during fermentation of black tea broth (Kombucha). *International Food Research Journal* **19,** 153–158 (2012).

91. Amin, M. C. I. M., Ahmad, N., Halib, N. & Ahmad, I. Synthesis and characterization of thermo- and pH-responsive bacterial cellulose/acrylic acid hydrogels for drug delivery. *Carbohydrate Polymers* **88,** 465–473 (2012).

92. Fink, H.-P., Purz, H. J., Bohn, A. & Kunze, J. Investigation of the supramolecular structure of never dried bacterial cellulose. *Macromolecular Symposia* **120,** 207–217 (1997).

93. Wei, B., Yang, G. & Hong, F. Preparation and evaluation of a kind of bacterial cellulose dry films with antibacterial properties. *Carbohydrate Polymers* **84,** 533–538 (2009).

94. Ford, E. N. J., Mendon, S. K., Thames, S. F. & Rawlins, J. W. X-ray Diffraction of Cotton Treated with Neutralized Vegetable Oil-based Macromolecular Crosslinkers. *Journal of Engineered Fibers and Fabrics* **5,** 10–20 (2010).

95. He, G. *et al.* Preparation, characterization and properties of aminoethyl chitin hydrogels. *Carbohydrate Polymers* **90,** 1614–1619 (2012).

96. Marek, S. R., Conn, C. A. & Peppas, N. A. Cationic Nanogels Based On Diethylaminoethyl Methacrylate. *Polymer* **51,** 1237–1243 (2010).

97. Levchik, G. F., Si, K., Levchik, S. V., Camino, G. & Wilkie, C. A. The correlation between cross-linking and thermal stability: Cross-linked polystyrenes and polymethacrylates. *Polymer Degradation and Stability* **65,** 395–403 (1999).

98. Tomé, L. C. *et al.* Preparation and characterization of bacterial cellulose membranes with tailored surface and barrier properties. *Cellulose* **17,** 1203–1211 (2010).

99. Cervantes-Uc, J. M., Cauich-Rodríguez, J. V., Herrera-Kao, W. A., Vázquez-Torres, H. & Marcos-Fernández, A. Thermal degradation behavior of polymethacrylates containing amine side groups. *Polymer Degradation and Stability* **93,** 1891–1900 (2008).

100. Abdellaoui-Arous, N. & Djadoun, S. Poly[2-(N,N-Dimethylamino) Ethyl Methacrylate] / Poly(Styrene-Co-Methacrylic Acid) Interpolymer Complexes. *Macromolecular Symposia* **303,** 123–133 (2011).

101. Luxila. at <http://2012.igem.org/Team:UC_Chile/Cyanolux/Project>

102. Watt, K., Christofi, N. & Young, R. The detection of antibacterial actions of whole herb tinctures using luminescent Escherichia coli. *Phytotherapy Research* **21,** 1193–1199 (2007).